Article

SOURCE DATA | TRANSPARENT PROCESS

THE EMBO JOURNAL

Caspase-8-driven apoptotic and pyroptotic crosstalk causes cell death and IL-1β release in X-linked inhibitor of apoptosis (XIAP) deficiency

Sebastian A Hughes[1,2,†], Meng Lin[3,4,†], Ashley Weir[1,2], Bing Huang[3], Liya Xiong[3], Ngee Kiat Chua[1,2], Jiyi Pang[1,2], Jascinta P Santavanond[5], Rochelle Tixeira[5], Marcel Doerflinger[1,2], Yexuan Deng[1,2], Chien-Hsiung Yu[1,2], Natasha Silke[1,2], Stephanie A Conos[6,7], Daniel Frank[1,2], Daniel S Simpson[1,2], James M Murphy[1,2], Kate E Lawlor[1,2,6,7], Jaclyn S Pearson[6,8], John Silke[1,2], Marc Pellegrini[1,2], Marco J Herold[1,2], Ivan K H Poon[5], Seth L Masters[1,2], Mingsong Li[9], Qin Tang[10], Yuxia Zhang[3,4,*], Maryam Rashidi[1,2,**], Lanlan Geng[3,4,***] & James E Vince[1,2,****]

Abstract

Genetic lesions in X-linked inhibitor of apoptosis (XIAP) pre-dispose humans to cell death–associated inflammatory diseases, although the underlying mechanisms remain unclear. Here, we report that two patients with XIAP deficiency–associated inflammatory bowel disease display increased inflammatory IL-1β maturation as well as cell death–associated caspase-8 and Gasdermin D (GSDMD) processing in diseased tissue, which is reduced upon patient treatment. Loss of XIAP leads to caspase-8-driven cell death and bioactive IL-1β release that is only abrogated by combined deletion of the apoptotic and pyroptotic cell death machinery. Namely, extrinsic apoptotic caspase-8 promotes pyroptotic GSDMD processing that kills macrophages lacking both inflammasome and apoptosis signalling components (caspase-1, -3, -7, -11 and BID), while caspase-8 can still cause cell death in the absence of both GSDMD and GSDME when caspase-3 and caspase-7 are present. Neither caspase-3 and caspase-7-mediated activation of the pannexin-1 channel, or GSDMD loss, prevented NLRP3 inflammasome assembly and consequent caspase-1 and IL-1β maturation downstream of XIAP inhibition and caspase-8 activation, even though the pannexin-1 channel was required for NLRP3 triggering upon mitochondrial apoptosis. These findings uncouple the mechanisms of cell death and NLRP3 activation resulting from extrinsic and intrinsic apoptosis signalling, reveal how XIAP loss can co-opt dual cell death programs, and uncover strategies for targeting the cell death and inflammatory pathways that result from XIAP deficiency.

Keywords caspase-8; Gasdermin D; inflammasome; pyroptosis; XIAP
Subject Categories Autophagy & Cell Death; Immunology
DOI 10.15252/embj.2021110468 | Received 17 December 2021 | Revised 8 December 2022 | Accepted 19 December 2022 | Published online 17 January 2023
The EMBO Journal (2023) 42: e110468

Introduction

X-linked inhibitor of apoptosis protein (XIAP), and the closely related cellular IAPs (cIAP1/2), are RING E3 ubiquitin ligases that were first described in mammals for their roles in suppressing apoptotic cell death (Duckett *et al*, 1996; Liston *et al*, 1996; Uren *et al*, 1996; Silke & Vince, 2017). However, recent evidence has placed XIAP as having a critical role in regulating pathogen-induced inflammatory responses, as humans with genetic lesions in XIAP (*Birc4*) are predisposed to the hyperinflammatory syndrome X-linked

1 The Walter and Eliza Hall Institute of Medical Research, Parkville, Vic, Australia
2 The Department of Medical Biology, University of Melbourne, Parkville, Vic, Australia
3 Department of Gastroenterology, Guangzhou Women and Children's Medical Center, Guangzhou, China
4 State Key Laboratory of Respiratory Medicine, Guangzhou Medical University, Guangzhou, China
5 Department of Biochemistry and Genetics, La Trobe Institute for Molecular Science, La Trobe University, Melbourne, Vic, Australia
6 Centre for Innate Immunity and Infectious Diseases, Hudson Institute of Medical Research, Clayton, Vic, Australia
7 Department of Molecular and Translational Science, Monash University, Clayton, Vic, Australia
8 Department of Microbiology, Monash University, Clayton, Vic, Australia
9 Department of Gastroenterology, The Third Affiliated Hospital of Guangzhou Medical University, Guangzhou, China
10 The First Affiliated hospital of Guangxi Medical University, Nanning, China
*Corresponding author. Tel: +86-188-2041-2127; E-mail: yuxia.zhang@gwcmc.org
**Corresponding author. Tel: +61-3-9345-2555; E-mail: rashidi@wehi.edu.au
***Corresponding author. Tel: +86-189-0226-8612; E-mail: 2012690086@gzhmu.edu.cn
****Corresponding author. Tel: +61-3-9345-2555; E-mail: vince@wehi.edu.au
†These authors contributed equally to this work as first authors

hemophagocytic lymphohistiocytosis (HLH), as well as inflammatory bowel conditions often resembling Crohn's disease (CD) (Marsh *et al*, 2010; Aguilar *et al*, 2014; Speckmann & Ehl, 2014; Wada *et al*, 2014; Aguilar & Latour, 2015; Zeissig *et al*, 2015; Amininejad *et al*, 2018). Other clinical manifestations resulting from the inheritance of XIAP mutations have also been described, including renal, dermatological, hepatic, pulmonary, infectious, neurological and musculoskeletal conditions (Mudde *et al*, 2021). Similar pathogenic variants of cIAP1/2 (*Birc2/3*) have not been reported, although studies show that cIAP degradation caused by toll-like receptor (TLR) and TNF signalling is key for the inflammatory and cell death responses in the context of XIAP deficiency (Vince *et al*, 2012; Wong *et al*, 2014; Lawlor *et al*, 2017; Knop *et al*, 2019). Indeed, small molecule drugs designed to mimic the IAP-binding motif of mitochondrial DIABLO/SMAC to antagonise XIAP and cIAPs (Du *et al*, 2000; Verhagen *et al*, 2000), phenocopy the cell death and inflammatory signalling triggered upon genetic XIAP deletion (Vince *et al*, 2012; Yabal *et al*, 2014; Lawlor *et al*, 2015, 2017).

The normal development of XIAP-deficient mice and human carriers of XIAP variants highlights that an environmental trigger, such as microbes, is likely to cause disease onset. Consistent with this idea, X-linked HLH is frequently triggered by pathogen infections, particularly Epstein–Barr virus, and is marked clinically by a range of symptoms, such as periodic fevers, hepatosplenomegaly, hyperferritinaemia, hypercytokinaemia and hemophagocytosis (Marsh *et al*, 2010; Wada *et al*, 2014; Aguilar & Latour, 2015). X-linked HLH is a fulminant and rapidly fatal disease, and the only cure is allogenic haematopoietic stem cell transplantation with reduced intensity conditioning, which carries a high risk of post-transplant mortality (Arico *et al*, 1996; Tang & Xu, 2011; Janka, 2012).

XIAP deficiency also causes inflammatory bowel disease (IBD) (Worthey *et al*, 2011; Amininejad *et al*, 2018). In fact, up to 4% of male paediatric patients with CD contain mutations in XIAP (Zeissig *et al*, 2015), and variants in XIAP have also been reported to cause adult-onset IBD (Quaranta *et al*, 2018; Parackova *et al*, 2020). The life-long debilitating symptoms of IBD result from an inappropriate mucosal immune response that has been linked to intestinal epithelial erosion and cell death and can result in diverse extraintestinal manifestations in many organ systems (Nunes *et al*, 2014; Patankar & Becker, 2020; Strigli *et al*, 2021; Wahida *et al*, 2021). CD caused by XIAP loss is particularly severe, with patients often being treatment-refractive and dying within a few years of onset or diagnosis (Nielsen & LaCasse, 2017; Chang *et al*, 2021). Hence, there is a significant need to unravel the mechanisms by which XIAP deficiency predisposes to heightened pathological inflammatory responses and cell death, both systemically and within the diseased tissue.

Patients with X-Linked HLH, or the related autoinflammatory condition, macrophage activation syndrome, exhibit sustained elevated levels of the inflammatory cytokines IL-18 and/or IL-1β (Wada *et al*, 2014; Weiss *et al*, 2018; Crayne *et al*, 2019). Systemic elevation of IL-18 and IL-1β are markers of inflammasome activation, which are pathologically triggered in numerous hereditary and environmentally associated autoinflammatory conditions (Canna *et al*, 2017; Manthiram *et al*, 2017; Rashidi *et al*, 2020; Speir & Lawlor, 2021). Under normal circumstances, the inflammasome sensor proteins, such as the NOD-like receptors (NLRs) NLRP1, NLRP3 and NLRC4, act to detect pathogen- or host-derived danger molecules to facilitate the innate and adaptive immune response (Menu & Vince, 2011; Jones *et al*, 2016). When activated, the NLR sensor forms a large multimeric cytosolic protein complex, an inflammasome, that triggers caspase-1 to process pro-IL-1β and pro-IL-18 into their bioactive forms. Caspase-1 simultaneously cleaves the pyroptotic cell death effector Gasdermin-D (GSDMD) and liberates its N-terminal fragment that forms pores in the plasma membrane, allowing the efficient egress of active IL-1β and IL-18 (Shi *et al*, 2015; Kayagaki *et al*, 2015b; Aglietti *et al*, 2016; Gaidt & Hornung, 2016; Sborgi *et al*, 2016).

We and other groups have previously demonstrated that in response to pathogen ligands and TLR signalling, or upon TNF-driven tumour necrosis factor receptor 1 (TNFR1) stimulation, murine XIAP deletion licences dendritic cell, macrophage and neutrophil extrinsic apoptotic caspase-8 activation (Vince *et al*, 2012; Yabal *et al*, 2014; Wicki *et al*, 2016; Knop *et al*, 2019). Activated caspase-8 can process precursor IL-1β directly in addition to inducing NLRP3 inflammasome formation to allow for caspase-1-mediated cleavage of IL-1β into its bioactive fragment (Maelfait *et al*, 2008; Vince *et al*, 2012; Yabal *et al*, 2014; Lawlor *et al*, 2015). However, the mechanisms underpinning the inflammatory functions of caspase-8 in the context of XIAP deficiency, including how it triggers NLRP3 activity and how it signals innate immune cell death, remain unclear.

Here we discover that two human patients with XIAP deficiency, presenting with IBD, exhibit heightened caspase-8-activation correlating with increased IL-1β and GSDMD processing in peripheral blood mononuclear cells (PBMCs) and inflamed colonic mucosae. Using IAP antagonist targeting to model XIAP deficiency we identify that extrinsic caspase-8 activates multiple downstream apoptotic and pyroptotic effectors, which act redundantly to cause both excess cell death and inflammatory IL-1β release. We further show that the pannexin-1 channel and GSDMD are not required for NLRP3 inflammasome assembly downstream of caspase-8, even though pannexin-1 is critical for NLRP3 signalling following mitochondrial apoptosis-mediated caspase-3 and caspase-7 activation. Collectively, these findings reveal redundancy in the mechanisms by which caspase-8 can induce IL-1β egress upon XIAP loss, identify potential therapeutic targets for treating X-linked HLH and IBD, and uncouple the downstream signalling events of intrinsic and extrinsic apoptosis that drive cell death and NLRP3 inflammasome responses.

Results

Processed caspase-8, GSDMD and IL-1β are increased in patients with XIAP-deficiency-associated inflammatory bowel disease

We performed whole exome sequencing and identified two male patients with XIAP deficiency. Patient 1 was a 9-year-old male with CD who had inherited a frameshift mutation (c.T993del-AGAAC: p.L331delE?) from his mother (Figs 1A and EV1A). An older brother of this patient had died from CD at the age of nine (Fig 1A). Patient 2 was a 1-year-old male presenting with Very Early Onset Inflammatory Bowel Disease (VEOIBD), who had inherited a missense mutation leading to a premature stop codon in XIAP (c595C>T:p.Q199X) (Figs 1A and EV1A). In both cases, colonoscopy examinations revealed erosions, ulcers and nodularity in the colon of both

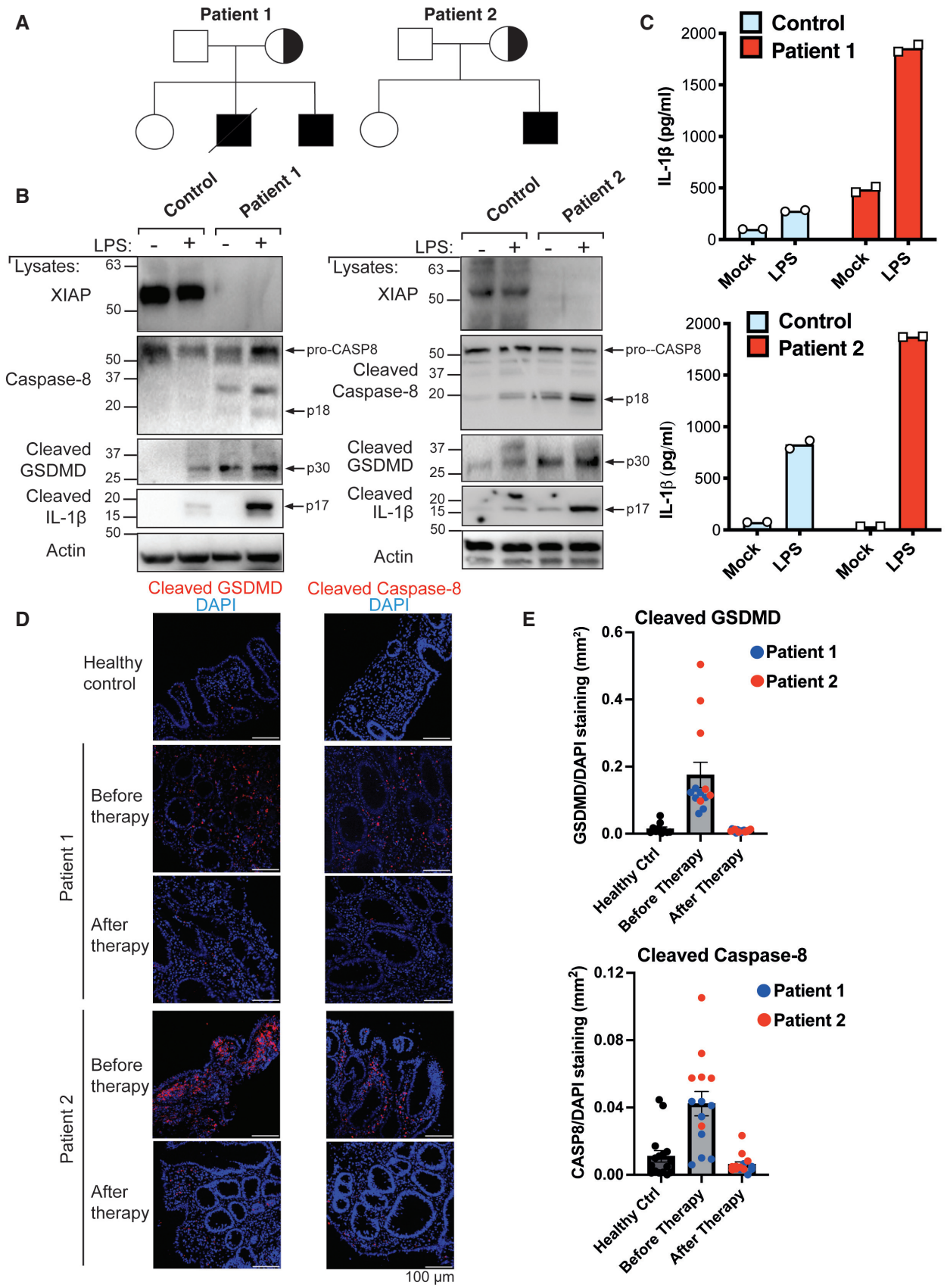
A
Patient 1
Patient 2
B
Control
Patient 1
LPS: - + - +
Lysates:
XIAP
Caspase-8
pro-CASP8
p18
Cleaved GSDMD
p30
Cleaved IL-1β
p17
Actin
Control
Patient 2
Cleaved Caspase-8
pro--CASP8
C
Control
Patient 1
IL-1β (pg/ml)
Mock
LPS
Control
Patient 2
D
Cleaved GSDMD
DAPI
Cleaved Caspase-8
Healthy control
Patient 1
Before therapy
After therapy
Patient 2
100 μm
E
Cleaved GSDMD
GSDMD/DAPI staining (mm²)
Patient 1
Patient 2
Healthy Ctrl
Before Therapy
After Therapy
Cleaved Caspase-8
CASP8/DAPI staining (mm²)

Figure 1.

Figure 1. XIAP deficiency in humans is associated with increased caspase-8, GSDMD and IL-1β activation.

A Pedigrees of the XIAP-deficient patients identified in this study.

B, C PBMCs were stimulated with LPS (500 ng/ml) and after 24 h cell lysates and supernatants analysed by western blot (B) and ELISA (C), respectively. The mean of experimental duplicates (symbols) is shown (C).

D, E Immunofluorescence staining showing activation of caspase-8 and GSDMD in the colonic mucosae of XIAP-deficient patients relative to healthy control colonic biopsies before and after early enteral nutrition (patient 1) or anti-TNF and immune suppression (patient 2) therapies, with several images (symbols) quantified in panel E (mean ± SEM of caspase-8 or GSDMD stained area relative to overall tissue staining (DAPI) analysed using ImageJ software. Caspase-8 staining quantified from; $n = 16$ healthy control, $n = 8$ and 6 before therapy (patient 1 and 2, respectively) and $n = 5$ and 9 after therapy (patient 1 and 2, respectively) separate images. GSDMD staining quantified from; $n = 10$ healthy control, $n = 7$ and 6 before therapy (patient 1 and 2, respectively) and $n = 8$ and 8 after therapy (patient 1 and 2, respectively) separate images.

Source data are available online for this figure.

patients (Fig EV1B). Western blot analysis of PBMCs revealed a complete loss of XIAP expression at the protein level in the two patients (Fig 1B). XIAP is required for NOD2 signalling (Krieg *et al*, 2009; Damgaard *et al*, 2012), and consistent with the lack of XIAP protein expression, muramyl dipeptide (MDP)-mediated activation of NOD2 to induce TNF and IL-6 secretion was defective in PBMCs from both XIAP-deficient patients compared with PBMCs from healthy donors (Fig EV1C and D).

Findings in mice indicate that the loss of XIAP increases TLR-induced caspase-8 activity to allow for cell death and cleavage of IL-1β into its 17 kDa bioactive fragment, which is released into the extracellular milieu (Vince *et al*, 2012; Yabal *et al*, 2014; Lawlor *et al*, 2017). However, whether the same signalling pathway is relevant to humans lacking XIAP, and in what tissues or cell types, remains unclear. Consistent with murine studies, XIAP-deficient patient PBMCs stimulated with LPS resulted in increased IL-1β egress compared with healthy control cells, as measured by ELISA (Fig 1C). Importantly, western blot analysis demonstrated that XIAP deficiency enhanced LPS-mediated cleavage of IL-1β into its bioactive form (p17), and this correlated with increased activation-associated caspase-8 processing and the cleavage of inflammasome-associated GSDMD into its pore-forming p30 fragment (Fig 1B).

To examine if the diseased colon of XIAP-deficient patients also displayed signs of cell death, the colonic mucosae of XIAP-deficient patients and healthy control subjects was stained for levels of cleaved and activated caspase-8 and GSDMD. Immunostaining and scoring of the colonic mucosae revealed that both XIAP-deficient patients exhibited increased levels of both active caspase-8 and GSDMD compared with healthy control colon samples (Figs 1D and E, and EV1E). Moreover, upon treatment (early enteral nutrition in patient 1 and anti-TNF and immune suppression in patient 2), the levels of cleaved caspase-8 and GSDMD detected in both patients were substantially reduced (Fig 1D and E).

Taken together, these data provide evidence that XIAP deficiency can predispose humans to increased TLR-driven caspase-8, GSDMD and IL-1β activation, in PBMCs and inflamed colonic mucosal tissue.

GSDMD is activated upon XIAP inhibition in the absence of caspase-1 and NLRP3

We next sought to model XIAP deficiency through the use of small molecule IAP antagonist (smac-mimetic) compounds. Although TLR and/or TNF-induced cIAP degradation is required for the IL-1β activation and macrophage death that can result from XIAP loss (Lawlor *et al*, 2017), the loss of cIAPs alone does not suffice to cause these responses (Lawlor *et al*, 2015). Consistent with these studies, only IAP antagonists that inhibit XIAP and cIAPs efficiently (Cp.A, 030, 031, 455) caused high levels of macrophage death, caspase-8 processing and associated caspase-1 and IL-1β activation, while those with selectivity for cIAPs (711 [birinapant], 851 and 883), did not (Figs 2A and EV1F and G) (Condon *et al*, 2014; Lawlor *et al*, 2015). Therefore, XIAP deficiency can be modelled in cells by treatment with bivalent IAP antagonists, such as Compound A (Cp. A), which target XIAP and cIAPs (Vince *et al*, 2007).

Our analysis of patient samples suggested that XIAP deficiency results in a caspase-8-GSDMD axis that facilitates IL-1β maturation and release to promote inflammatory responses (Fig 1). In addition to caspase-8 engagement of the NLRP3 inflammasome to activate caspase-1 (Lawlor *et al*, 2015; Gaidt *et al*, 2016), recent studies have indicated that caspase-8 can also directly process GSDMD to drive pyroptotic cell death (Orning *et al*, 2018; Sarhan *et al*, 2018; Demarco *et al*, 2020; Muendlein *et al*, 2020). However, caspase-1 is reported to be more efficient at cleaving GSDMD than caspase-8 (Shi *et al*, 2015; Orning *et al*, 2018).

To assess whether caspase-8 contributes to GSDMD activity in XIAP deficiency via NLRP3-caspase-1 activation or direct caspase-8 processing, we primed bone marrow–derived macrophages (BMDMs) from wild-type (WT), *Nlrp3*$^{-/-}$ and *Caspase-1*$^{-/-}$ mice with LPS and treated them with Cp. A to phenocopy XIAP loss and pathogen challenge. Consistent with our analysis of XIAP-deficient patients, Cp. A treatment resulted in the processing of GSDMD into its active p30 fragment (Fig 2B). Although reduced, GSDMD activation was still detected in both *Nlrp3*$^{-/-}$ and *Caspase-1*$^{-/-}$ BMDMs following Cp. A treatment, which correlated with the processing of caspase-8 (Fig 2B). This contrasted to the treatment of BMDMs with the canonical NLRP3 stimuli, nigericin, which triggered the production of active GSDMD in a NLRP3- and caspase-1-dependent manner (Fig 2B). In line with previous findings (Vince *et al*, 2012; Lawlor *et al*, 2015), Cp. A also activated the NLRP3 inflammasome, as its ability to induce caspase-1 processing to the p20 fragment was abrogated in *Nlrp3*$^{-/-}$ (and *Caspase-1*$^{-/-}$) BMDMs. On the other hand, Cp. A-induced IL-1β activation and release was only modestly compromised by the loss of NLRP3 signalling; a result of caspase-8 processing IL-1β directly (Fig 2B) (Maelfait *et al*, 2008; Vince *et al*, 2012).

To help understand if IAP inhibition, associated caspase-8 processing, and consequent NLRP3, GSDMD and IL-1β activation were mirrored by other agents that trigger caspase-8, we treated LPS

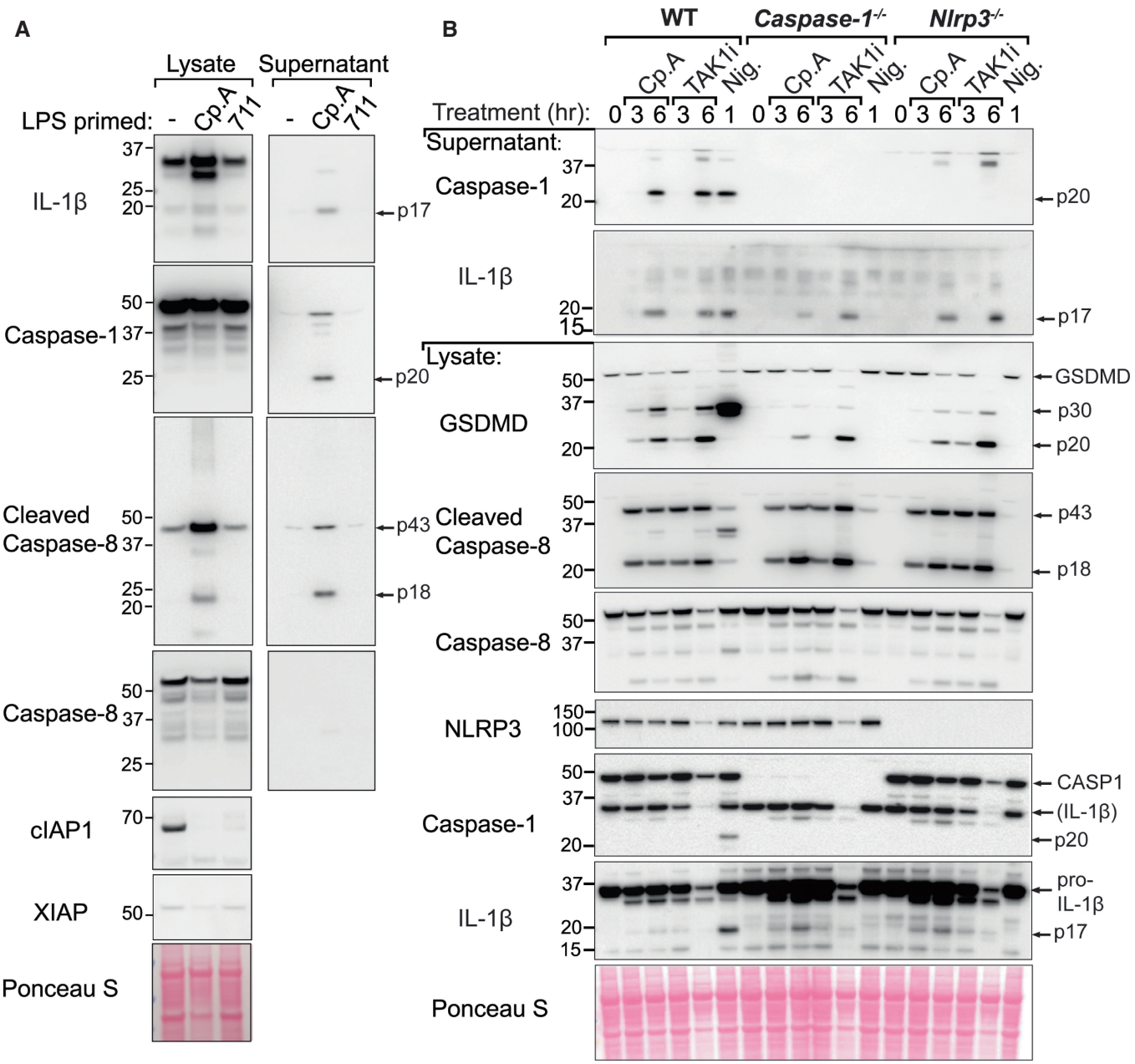

Figure 2. GSDMD is processed upon IAP targeting even in the absence of caspase-1 or NLRP3.

A BMDMs were seeded at a density of 4×10^5 cells per well, primed with 20 ng/ml of LPS for 3 h then treated, as indicated, with 500 nM of Cp. A or 711 for 20 h and cell lysates and supernatants were analysed by western blot. Ponceau staining depicts protein loading. Data representative of two independent experiments.

B BMDMs of the indicated genotypes were seeded at a density of 5×10^5 cells per well and primed with 100 ng/ml of LPS for 3 h then treated, as indicated, with Cp. A (1 μM), 5Z-7 oxozeaenol (TAK1i, 250 nM) for 3 or 6 h or nigericin (10 μM) for 45 min. Cell lysates and supernatants were analysed by western blot. Ponceau staining depicts protein loading. Data representative of two independent experiments.

Source data are available online for this figure.

primed BMDMs with the TAK1 inhibitor (5Z)-7-Oxozeaenol (TAK1i), as TAK1 is required to prevent caspase-8-dependent cell death (Lluis *et al*, 2010; Sarhan *et al*, 2018). Akin to Cp. A treatment, the inhibition of TAK1 induced caspase-8 activation and NLRP3-mediated caspase-1 processing and IL-1β maturation (Fig 2B). Importantly, TAK1 inhibition also resulted in cleavage of GSDMD into the p30 pore-forming fragment in both *Nlrp3*$^{-/-}$ and *Caspase-1*$^{-/-}$ BMDMs (Fig 2B). Therefore, in macrophages, IAP loss and TAK1 inhibition trigger an inflammatory signalling pathway initiated by caspase-8.

GSDMD and GSDME are not required for cell death or IL-1β secretion upon XIAP inhibition

Recent studies have reported that upon TAK1 inhibition, caspase-8 activates the pore-forming protein GSDMD to promote cell death and allow IL-1β release (Orning *et al*, 2018; Sarhan *et al*, 2018; Demarco *et al*, 2020; Muendlein *et al*, 2020). Given the increased GSDMD activation observed in XIAP-deficient patients (Fig 1), and the similarities in the caspase-8-driven inflammatory response between TAK1 and XIAP-inhibited cells (Fig 2), we hypothesised that GSDMD would also contribute to cell death and IL-1β release following the loss of XIAP function.

WT and *Gsdmd*$^{-/-}$ BMDMs were primed with LPS before treatment with Cp. A for 4, 8 and 16 h. Surprisingly, the loss of GSDMD did not impact Cp. A-mediated cell death at either early or late time points, even in the presence of the NLRP3 inflammasome inhibitor, MCC950 (Coll *et al*, 2015) (Fig 3A). On the other hand, and as expected (Shi *et al*, 2015), GSDMD loss or the inhibition of NLRP3 with MCC950 limited nigericin-induced macrophage killing (Fig 3A). To further tease apart more discrete differences in cell death kinetics upon GSDMD loss we employed IncuCyte live cell imaging analysis. In line with our flow cytometric analysis, the loss of GSDMD had little impact on the rate of cell death upon treatment with Cp. A or TAK1i with or without the addition of MCC950 (Fig EV2A–C). Deletion of GSDMD also did not alter Cp. A triggered release of IL-1β (or TNF) as measured by ELISA (Fig 3B and C), although MCC950 targeting of NLRP3 did moderately reduce IL-1β egress (Fig 3B), as expected based on genetic studies (Vince *et al*, 2012). In line with these findings, western blotting showed that the abundance of cleaved, bioactive IL-1β in the cell supernatants upon IAP inhibition was not impacted by GSDMD deletion (Fig 3D). Additionally, we observed that Cp. A treatment caused comparable levels of cleaved caspase-8 to be released from WT and GSDMD-deficient cells, consistent with equivalent cell death responses between these genotypes (Fig 3D).

Caspase-8 activates caspase-3 which in turn can cleave GSDME to elicit pyroptotic cell death (Rogers *et al*, 2017; Wang *et al*, 2017). GSDME may also contribute to pathological NLRP3 inflammasome responses that are mediated by caspase-8 (Wang *et al*, 2021). We, therefore, reasoned that GSDME, either alone or in combination with GSDMD, could have a role in cell death and IL-1β release following the loss of IAP function and consequent caspase-8 processing. However, like the genetic deletion of GSDMD, the deletion of GSDME alone, or together with GSDMD, did not impact Cp. A-mediated cell death kinetics (Figs 3A and EV2A–C), IL-1β (or TNF) release (Fig 3B and C), nor the accumulation of bioactive IL-1β in the cell supernatants (Fig 3D). Moreover, IL-1β was still released upon NLRP3 inhibition with MCC950 (which blocked all caspase-1 processing) equivalently in WT, *Gsdme*$^{-/-}$ and *Gsdmd*$^{-/-}$*Gsdme*$^{-/-}$ BMDMs (Fig 3B and D). Therefore, when IAP function is compromised, GSDMD and GSDME are not required for caspase-8-mediated IL-1β proteolysis and release, nor cell death, either in the presence or the absence of caspase-1 activity.

GSDMD deletion compromises bioactive IL-1β release but not cell death upon TAK1 inhibition

Given that bioactive IL-1β release upon XIAP inhibition did not depend on GSDMD, we re-evaluated the proposed role for caspase-8-mediated GSDMD cleavage in cell death and IL-1β release upon TAK1 inhibition (Orning *et al*, 2018; Sarhan *et al*, 2018; Muendlein *et al*, 2020). As expected, TAK1 inhibition efficiently reduced LPS-mediated signalling, as shown by reduced phosphorylation of ERK1/2 and p38 (Fig EV2D). Surprisingly, examination of cell death via propidium iodide (PI) uptake (Fig 4A), or cell death kinetics in real time by IncuCyte imaging (Fig EV2E and F), revealed equitable responses in *Gsdmd*$^{-/-}$, *Gsdme*$^{-/-}$, *Gsdmd*$^{-/-}$*Gsdme*$^{-/-}$ and WT macrophages, regardless of the dose of TAK1 inhibitor used, or whether NLRP3 was also inhibited with MCC950.

Previous research implicating GSDMD in efficient cell death responses following TAK1 inhibition often used LDH as the cell death readout (Orning *et al*, 2018; Sarhan *et al*, 2018; Muendlein *et al*, 2020). However, the membrane rupture that allows LDH release can be uncoupled from cell death (Kayagaki *et al*, 2021). The delay in cell death kinetics previously reported between WT and GSDMD-deficient macrophages may result from the dose of TAK1 inhibitor used and/or differences in cell culture conditions known to impact macrophage-killing responses, such as cell density (Lawlor *et al*, 2017). Regardless, unlike the inhibition of IAPs with Cp. A, or the triggering of BAX and BAK-driven mitochondrial apoptosis with BH3-mimetic (ABT-737) and cycloheximide (CHX) treatment (Vince *et al*, 2018), the release of cleaved bioactive IL-1β into the cell supernatant was reduced upon GSDMD deletion in TAK1 inhibited macrophages (Fig 4B). Therefore, macrophages lacking TAK1 and IAP activity differ in their requirement for GSDMD pores to allow the efficient egress of bioactive IL-1β, although in both cases GSDMD is ultimately dispensable for cell death.

The deletion of GSDMD does not affect NLRP3-dependent ASC oligomerisation downstream of caspase-8

Akin to non-canonical caspase-11-GSDMD-driven activation of NLRP3 (Baker *et al*, 2015; Ruhl & Broz, 2015), the death ligand FasL has recently been reported to activate a caspase-8-GSDMD axis to allow for potassium ion efflux and consequentially trigger NLRP3 inflammasome activation (Donado *et al*, 2020). Intriguingly,

Figure 3. GSDMD and GSDME are not required for cell death or IL-1β release upon IAP inhibition.

A–C BMDMs (5×10^5 cells per well) of the indicated genotypes were primed with 100 ng/ml of LPS for 3 h before treatment with Cp. A (1 μM, up to 16 h as indicated) or nigericin (10 μM) for 20 min, in the absence or presence of the NLRP3 inhibitor MCC950 (5 μM). (A) Cell viability was measured through propidium iodide (PI) uptake and flow cytometry and expressed as a proportion of PI negative (live) cells. (B and C) IL-1β (B) and TNF (C) levels in cell supernatants were measured by ELISA at the 6 h time point. Data for (A–C) represent the mean of three independent experiments (symbols) and error bars represent the mean ± SD.

D BMDMS of the indicated genotypes were treated as in A, and cell lysates and supernatants analysed by western blot. Representative of three independent experiments.

Source data are available online for this figure.

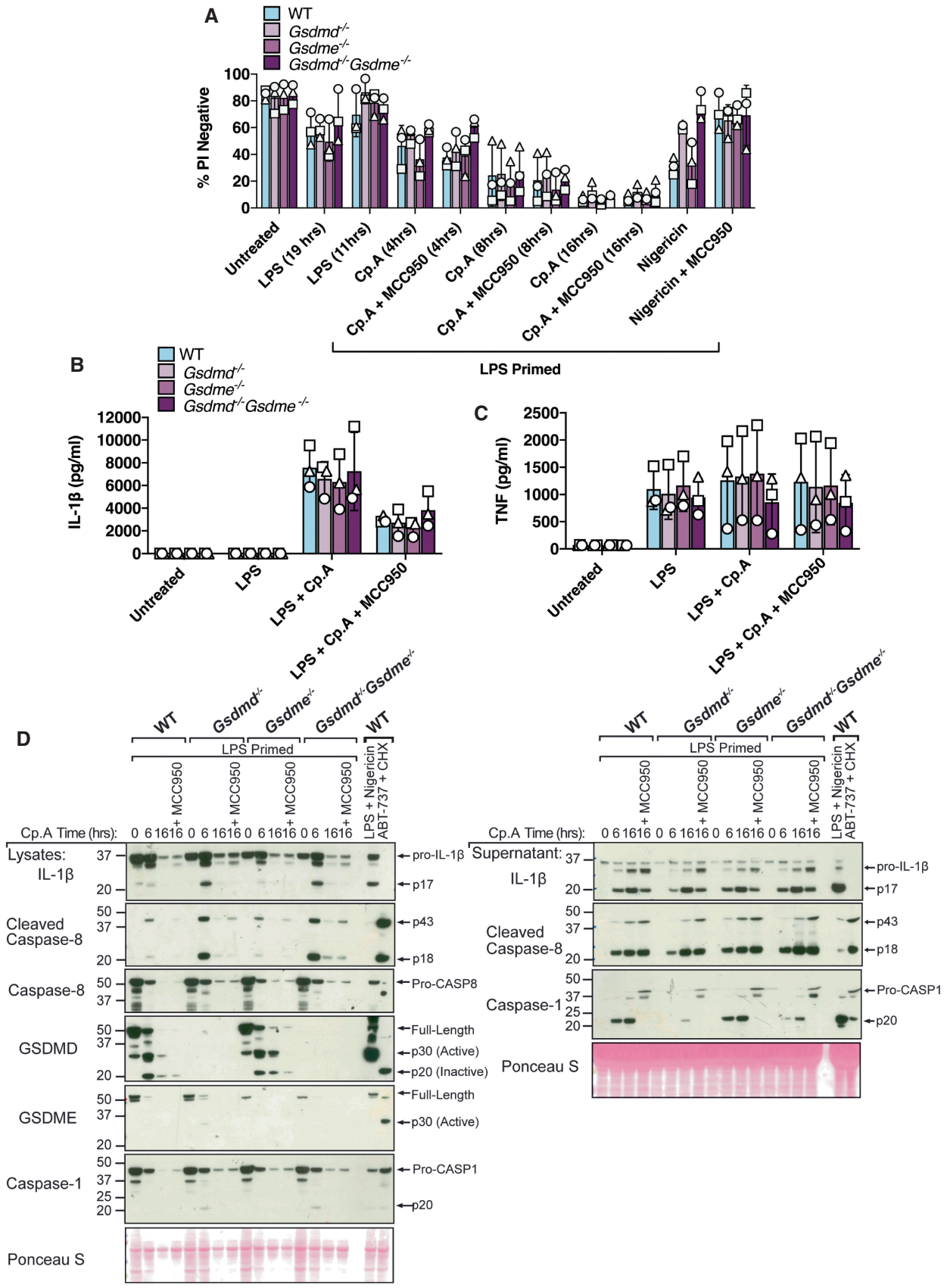
A
WT
Gsdmd-/-
Gsdme-/-
Gsdmd-/-Gsdme-/-
% PI Negative
Untreated
LPS (19 hrs)
LPS (11hrs)
Cp.A (4hrs)
Cp.A + MCC950 (4hrs)
Cp.A (8hrs)
Cp.A + MCC950 (8hrs)
Cp.A (16hrs)
Cp.A + MCC950 (16hrs)
Nigericin
Nigericin + MCC950
LPS Primed
B
IL-1β (pg/ml)
Untreated
LPS
LPS + Cp.A
LPS + Cp.A + MCC950
C
TNF (pg/ml)
D
LPS Primed
+ MCC950
LPS + Nigericin ABT-737 + CHX
Cp.A Time (hrs): 0 6 16 16
Lysates: IL-1β
pro-IL-1β
p17
Cleaved Caspase-8
p43
p18
Caspase-8
Pro-CASP8
GSDMD
Full-Length
p30 (Active)
p20 (Inactive)
GSDME
Caspase-1
Pro-CASP1
Ponceau S
Supernatant: IL-1β

Figure 3.

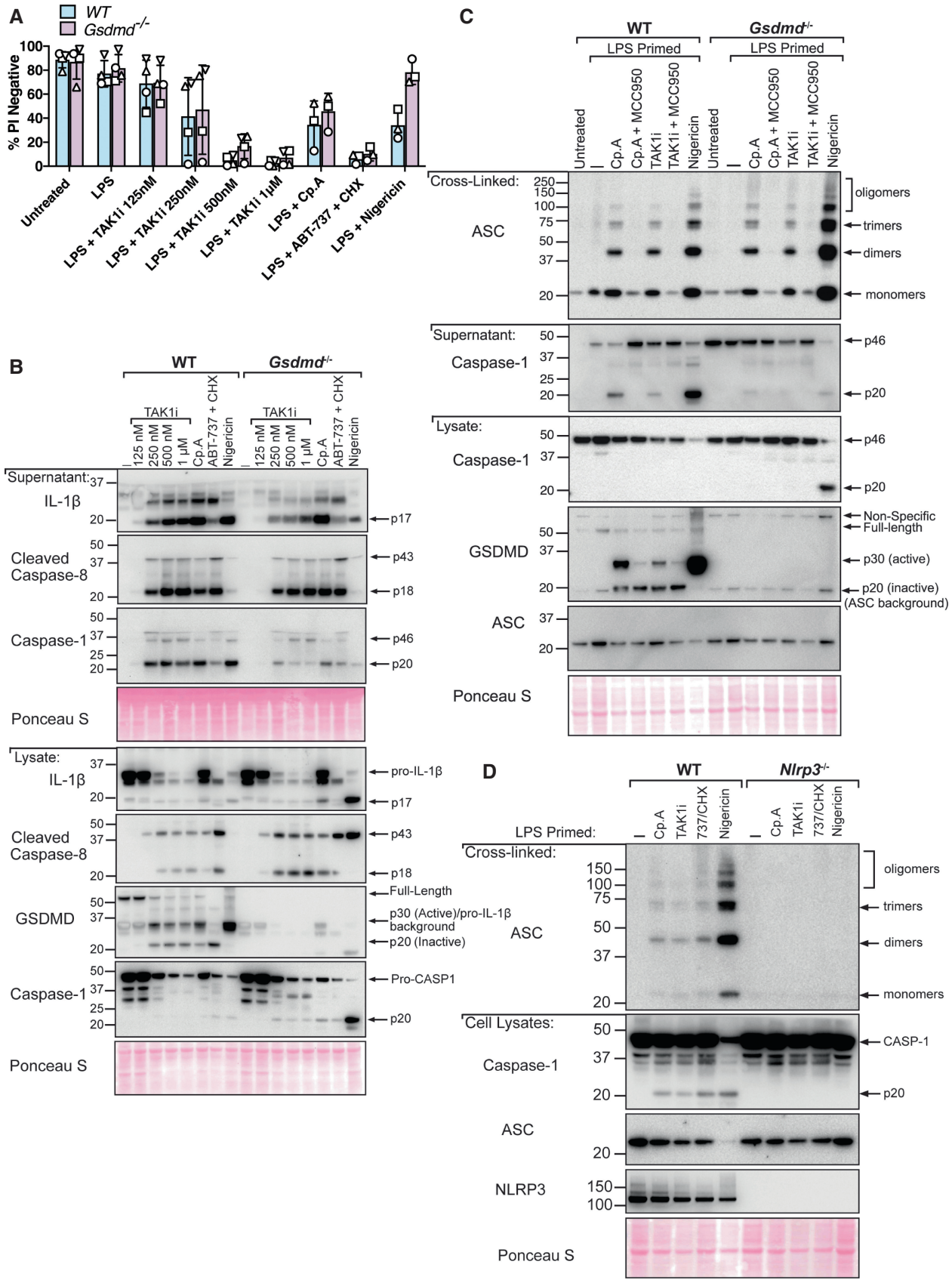

Figure 4.

Figure 4. GSDMD is dispensable for NLRP3-mediated ASC oligomerisation downstream of caspase-8.

A BMDMs of the indicated genotypes were primed with 100 ng/ml of LPS for 3 h before treatment with 5Z-7 oxozeaenol (TAK1i, 125 nM, 250 nM, 500 nM, and, 1 μM), Cp. A (1 μM) or ABT-737 (1 μM) and CHX (20 μg/ml) for 6 h, or nigericin (10 μM) for 20 min. Cell viability was measured by propidium iodide (PI) uptake and flow cytometry and expressed as a percentage of PI-negative (live) cells. Three to four independent experiments are shown (symbols), and error bars represent the mean ± SD.

B BMDMs of the indicated genotypes were primed with 100 ng/ml of LPS for 3 h before treatment with 5Z-7 oxozeaenol (TAK1i, 125 nM, 250 nM, 500 nM, and, 1 μM), Cp. A (1 μM) or ABT-737 (1 μM) and CHX (20 μg/ml) for 6 h, or nigericin (10 μM) for 45 min. Cell supernatants and total cell lysates were analysed by western blot. Ponceau staining depicts protein loading. One of three independent experiments.

C BMDMs of the indicated genotypes were seeded at a density of 2×10^6 cells per well and primed with LPS (100 ng/ml) for 3 h before treatment with Cp. A (1 μM) or 5Z-7 oxozeaenol (TAK1i, 250 nM) with or without the NLRP3 inhibitor MCC950 (5 μM) for 6 h or were treated with nigericin (10 μM) for 45 min. Cell lysates and supernatants were analysed by western blot. Following freeze-thawing of cells, the PBS-insoluble fraction of the cell lysate was cross-linked and assessed for ASC oligomerisation by western blot. Ponceau staining depicts protein loading. Data representative of three independent experiments.

D BMDMs of the indicated genotypes were seeded at a density of 2×10^6 cells per well and primed with 100 ng/ml LPS for 6 h before treatment with Cp. A (1 μM) or TAK1i (250 nM) for 6 h, ABT-737 (1 μM) and CHX (20 μg/ml) for 3 h and Nigericin (10 μM) for 1 h. PBS insoluble fractions of cell lysates were cross-linked to assess ASC oligomerisation and these, alongside cell lysates and supernatants, were analysed by western blot. Data represent two independent experiments.

Source data are available online for this figure.

western blot analysis of GSDMD-deficient macrophages treated with Cp. A or TAK1 inhibitor revealed a reduction in the release of the p20 fragment of caspase-1, indicating that GSDMD pores may also promote NLRP3-caspase-1 signalling under these conditions (Figs 3D and 4B). However, cell lysate analysis showed that some caspase-1 p20 can accumulate in cells upon GSDMD deletion (Figs 3D and 4B; Appendix Fig S1A) and, unlike NLRP3 inhibition, IL-1β release was not reduced upon GSDMD loss (Fig 3B and D). Therefore, these results make it difficult to establish if GSDMD loss prevents NLRP3-mediated caspase-1 activation upon IAP inhibition, or if a lack of GSDMD pore formation simply limits caspase-1 p20 release.

To better understand if GSDMD pores promote NLRP3 signalling in the context of IAP deficiency or TAK1 inhibition, we evaluated NLRP3 inflammasome formation directly via NLRP3-induced ASC oligomerisation. WT and *Gsdmd*$^{-/-}$ BMDMs were primed with LPS and then treated with Cp. A or TAK1 inhibitor for up to 6 h and ASC cross-linking assays performed. As expected, inhibition of NLRP3 in WT macrophages using MCC950, or genetic deletion of NLRP3, abrogated ASC oligomerisation downstream of IAP or TAK1 inhibition (Fig 4C and D; Appendix Fig S1). However, compared directly with WT cells, ASC oligomer profiling in GSDMD-deficient cells was not affected (Fig 4C and D). These results mirrored ASC oligomerisation patterns in WT and *Gsdmd*$^{-/-}$ BMDMs in response to treatment with the canonical NLRP3 activator nigericin (Fig 4C and D). Therefore, caspase-8-driven NLRP3 inflammasome formation occurs upstream of GSDMD activity in both IAP and TAK1 targeted cells.

Pannexin-1 is required for BAX/BAK-mediated activation of NLRP3 but is dispensable for NLRP3 inflammasome assembly downstream of caspase-8

The activation of the apoptotic effector caspases, caspase-3 and -7, can result in NLRP3 signalling (Chauhan *et al*, 2018; Vince *et al*, 2018). More recently, it has been suggested that NLRP3 triggering downstream of both intrinsic (BAX and BAK-mediated) and extrinsic (caspase-8-mediated) apoptosis is a consequence of caspase-3 and -7-dependent cleavage and activation of the hemichannel, pannexin-1, to allow potassium ion efflux (Chen *et al*, 2019). To test the role of pannexin-1 in caspase-8-dependent NLRP3 inflammasome assembly resulting from IAP loss, we generated Pannexin-1-deficient mice and mice harbouring a mutant Pannexin-1 that is unable to be cleaved and activated by caspase-3 and -7 (*Panx1*$^{nc/nc}$). Remarkably, ASC oligomerisation, as well as caspase-1 processing to its p20 fragment and cell death, were unaffected in both *Panx1*$^{-/-}$ and *Panx1*$^{nc/nc}$ BMDMs following Cp. A or TAK1 inhibitor treatment (Fig 5A–G; Appendix Fig S2). In contrast, both ASC oligomerisation and caspase-1-processing downstream of ABT-737/CHX-mediated BAX and BAK signalling were reduced in *Panx1*$^{-/-}$ and *Panx1*$^{nc/nc}$ BMDMs (Fig 5B; Appendix Fig S2), while nigericin responses were intact (Fig 5B). On the other hand, ABT-737/CHX-driven cell death

Figure 5. Pannexin-1 is required for BAX and BAK-mediated activation of NLRP3 but is dispensable for NLRP3 inflammasome assembly downstream of caspase-8.

A, B BMDMs of the indicated genotypes were seeded at a density of 2×10^6 cells per well and were primed with 100 ng/ml LPS for 3 h and then treated with Cp. A (1 μM) for 6 h (A) or with 5Z-7 oxozeaenol (TAK1i, 250 nM) or ABT-737 (1 μM) and CHX (20 μg/ml) for 6 h, or nigericin (10 μM) for 45 min (B). Cell lysates and supernatants were analysed by western blot and the PBS-insoluble fraction of the cell lysate was cross-linked and assessed for ASC oligomerisation by western blot. Ponceau staining depicts protein loading. Data representative of two independent experiments.

C BMDMs of the indicated genotypes were seeded at a density of 5×10^5 cells per well and were treated as outlined in (A) and (B). Cell viability was determined by PI staining and flow cytometry and measured as a proportion of PI-negative (live) cells. Data represent the mean of three to four independent experiments (symbols). Error bars are the mean ± SD.

D BMDMs of the indicated genotypes were seeded at a density of 5×10^5 cells per well and cell lysates were analysed by western blot.

E–G IncuCyte live cell imaging analysis of BMDM death kinetics. BMDMs were seeded at a density of 7.5×10^4 per well and primed with LPS (100 ng/ml) for 3 h before treatment with Cp.A (1 μM, E), TAK1i (250 nM, F) or ABT-737 (1 μM) + CHX (20 μg/ml, G) for 14 h. Cell death was measured as a percentage of cytox green positive cells versus SPY620-DNA positive cells. Each graph is representative of three independent experiments, data points represent the mean of triplicate wells. Error bars are the mean ± SD.

Source data are available online for this figure.

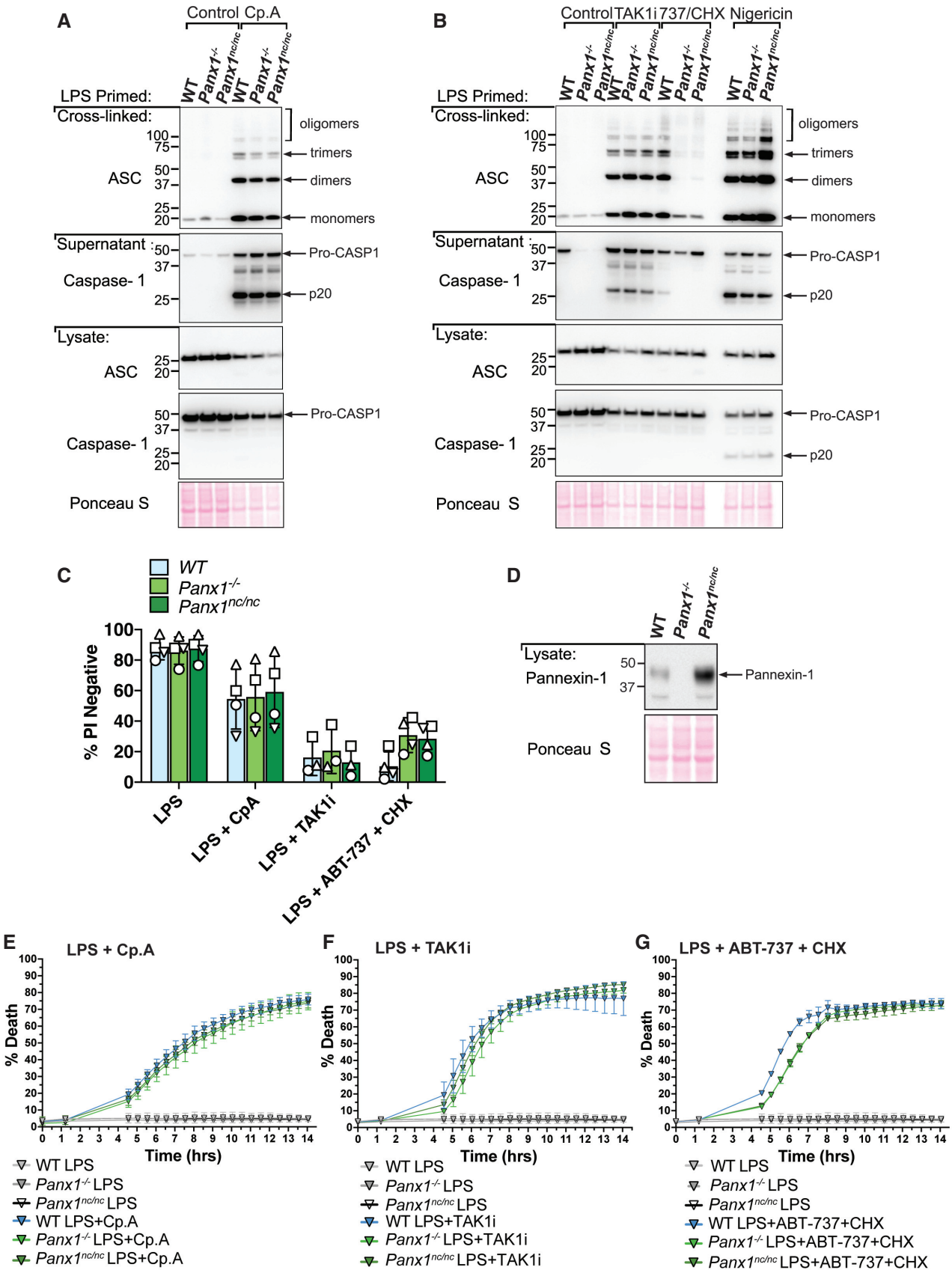

Figure 5.

was not prevented by pannexin-1 deletion or mutation of its caspase cleavage site (Fig 5C and G). Consequently, these data provide genetic evidence that caspase-3 and -7 cleave pannexin-1 to activate NLRP3 downstream of intrinsic mitochondrial apoptosis but that pannexin-1 cleavage is dispensable for NLRP3 inflammasome assembly downstream of extrinsic apoptotic caspase-8 and thus IAP deficiency.

The absence of caspase-1, −3, −7, −11 and BID does not alter cell death upon IAP inhibition

Despite evidence that caspase-8 may cleave GSDMD upon the loss of IAP function (Figs 1 and 2), we found that deletion of GSDMD and GSDME combined with the inhibition of NLRP3-caspase-1 had no impact on caspase-8-dependent macrophage killing following Cp. A treatment (Fig 3A). Caspase-8 processing of the apoptotic effector caspases, caspase-3 and caspase-7, is the best described mechanism for extrinsic cell death. Nevertheless, caspase-8 can also signal NLRP3-caspase-1 activation (Lawlor *et al*, 2015), can collaborate with caspase-11 to cause cell death (Mandal *et al*, 2018), can cleave BID to initiate mitochondrial apoptosis (Li *et al*, 1998), and inhibits RIPK3-driven necroptosis caused by the necroptotic effector MLKL (Alvarez-Diaz *et al*, 2016). Indeed, western blot analysis demonstrated that, in addition to caspase-1 (Fig 2), IAP targeting with Compound A or inhibition of TAK1 caused processing of caspase-3, −7 and − 9, and the cleavage of caspase-3 and -7, and/or caspase-9 still occurred in *Panx1*$^{-/-}$, *Panx*$^{nc/nc}$, *Nlrp3*$^{-/-}$, *Caspase-1*$^{-/-}$, *Gsdmd*$^{-/-}$, *Gsdme*$^{-/-}$, and *Gsdmd*$^{-/-}$*Gsdme*$^{-/-}$ macrophages (Fig EV3A–D). Therefore, to define whether several cell death pathways might work in conjunction to cause cell death upon IAP deficiency, we analysed CRISPR/Cas9 gene-targeted immortalised BMDMs (iBMDMs) with combined genetic deletion of the inflammatory caspases (caspase-1, -11 and -12), intrinsic (BID, caspase-9) and extrinsic (RIPK3, caspase-8, MLKL) death regulators, and the apoptotic effector caspases, caspase-3 and -7 (Aubrey *et al*, 2015; Doerflinger *et al*, 2020). Western blotting was used to confirm efficient deletion of the targeted genes (Appendix Fig S3). Strikingly, cell death resulting from LPS priming and Cp. A treatment of *Caspase-1*$^{-/-}$*3*$^{-/-}$*7*$^{-/-}$*11*$^{-/-}$*12*$^{-/-}$*Bid*$^{-/-}$*Mlkl*$^{-/-}$ iBMDMs occurred as efficiently as that observed in LPS and Cp. A treated WT iBMDMs, or in LPS stimulated XIAP-deficient macrophages (Fig 6A). As expected, *Caspase-1*$^{-/-}$*3*$^{-/-}$*7*$^{-/-}$*11*$^{-/-}$*12*$^{-/-}$*Bid*$^{-/-}$*Mlkl*$^{-/-}$ macrophages were protected from necroptosis (LPS/Cp. A/IDN-6556 treatment), pyroptosis (LPS/nigericin treatment) and intrinsic apoptosis (ABT-737/CHX treatment) (Fig 6B). In agreement with BID being dispensable for Cp. A-induced cell death (Fig 6A), BAX and BAK deficiency also did not alter macrophage killing resulting from IAP antagonism (Fig 6C), despite the protection of *Bax*$^{-/-}$*Bak*$^{-/-}$ iBMDMs to ABT-737 and CHX treatment (Fig 6C). Moreover, the lesser studied apoptotic effector caspase-6 could not substitute for caspase-3 and caspase-7 loss, as the genetic deletion of caspase-6 in combination with caspase-1,-3,-7,-11 and -12 did not alter macrophage killing, nor abrogate IL-1β activation, in response to LPS priming and Cp. A treatment (Fig EV4A and B). Concordant with these findings in macrophages, *Caspase-3*$^{-/-}$*Caspase-7*$^{-/-}$ murine embryonic fibroblasts (MEFs) were also susceptible to extrinsic cell death resulting from TNF and IAP antagonist treatment yet were protected from intrinsic BAX and BAK-mediated apoptosis caused by MCL-1 deletion combined with ABT-737 or etoposide treatment (Fig EV5A–C).

Collectively, these data reveal that extrinsic and intrinsic apoptosis differ in their requirement for caspase-3 and caspase-7 for inducing efficient cell death. Moreover, they genetically demonstrate that upon IAP loss, caspase-8 can kill in the combined absence of apoptotic caspase-3 and caspase-7, inflammatory caspases and necroptotic cell death signalling.

In the absence of caspase-1, -3, -7 and BID, caspase-8 can cleave GSDMD to cause cell death

We next considered that caspase-8 processing of GSDMD may be responsible for cell death in the absence of the apoptotic signalling machinery. We, therefore, generated *Caspase-1*$^{-/-}$*3*$^{-/-}$*7*$^{-/-}$*9*$^{-/-}$*Bid*$^{-/-}$*Mlkl*$^{-/-}$*Gsdmd*$^{-/-}$ iBMDMs (lacking caspase-1, -3, -7, BID, MLKL and GSDMD). Strikingly, these iBMDMs were completely protected from Cp. A-induced cell death (Fig 6A), unlike the efficient cell death observed in *Gsdmd*$^{-/-}$ and/or NLRP3 inhibited cells (Fig 3A and B) and macrophages lacking caspase-1, -3, -7 and BID (Fig 6A). Control cells lacking the essential extrinsic cell death machinery, RIPK3 and caspase-8 (*Caspase-3*$^{-/-}$*7*$^{-/-}$*8*$^{-/-}$*Bid*$^{-/-}$*Ripk3*$^{-/-}$*Mlkl*$^{-/-}$*Gsdmd*$^{-/-}$ iBMDMs), were also protected from Cp. A-mediated macrophage killing, as expected (Fig 6A) (Lawlor *et al*, 2015). In agreement with previous observations (Orning *et al*, 2018; Sarhan *et al*, 2018), we also found that the expression of caspase-8 in 293 T cells could phenocopy caspase-1 activity and cause the cleavage of FLAG-tagged GSDMD into its pore-forming p30 fragment (Fig EV5D). Taken together, these data indicate that caspase-8 can directly target GSDMD for proteolysis and activation and that in the absence of apoptotic signalling, caspase-8 signals through GSDMD to induce efficient cell death upon IAP targeting. Importantly, this points to a redundant role for pyroptotic and apoptotic death effectors in executing extrinsic cell death. In contrast, intrinsic BAX- and BAK-mediated apoptosis relies entirely on caspase-3 and caspase-7 for the efficient killing of macrophages and fibroblasts (Fig 6D).

In the absence of caspases-1, -3 and -7, XIAP inhibition triggers caspase-8-mediaed processing of IL-1β and GSDMD to allow for IL-1β activation and release

Considering (i) the redundant roles and crosstalk for apoptotic caspases and GSDMD in driving cell death, and (ii) that GSDMD and GSDME were dispensable for IL-1β secretion in the presence of caspase-3 and caspase-7 (Fig 3B and D), we hypothesised that caspase-8 can cleave GSDMD to allow for IL-1β release upon the loss of IAP function.

We first examined LPS-induced NLRP3 and precursor IL-1β expression in our multi-gene knockout iBMDMs to ensure any results did not reflect defects in TLR4 responses and inflammasome priming. Importantly, LPS priming induced efficient expression of both NLRP3 and IL-1β, as well as TNF, in WT, *Caspase-1*$^{-/-}$*3*$^{-/-}$*7*$^{-/-}$*11*$^{-/-}$*12*$^{-/-}$*Bid*$^{-/-}$*Mlkl*$^{-/-}$, *Caspase-1*$^{-/-}$*3*$^{-/-}$*7*$^{-/-}$*9*$^{-/-}$*Bid*$^{-/-}$*Mlkl*$^{-/-}$*Gsdmd*$^{-/-}$ and *Xiap*$^{-/-}$ iBMDMs (Fig 7A and B; Appendix Fig S4). These cells (unless genetically targeted) also expressed similar levels of the other inflammasome components, ASC, caspase-1 and caspase-8 (Appendix Fig S4). However, consistent with caspase-8

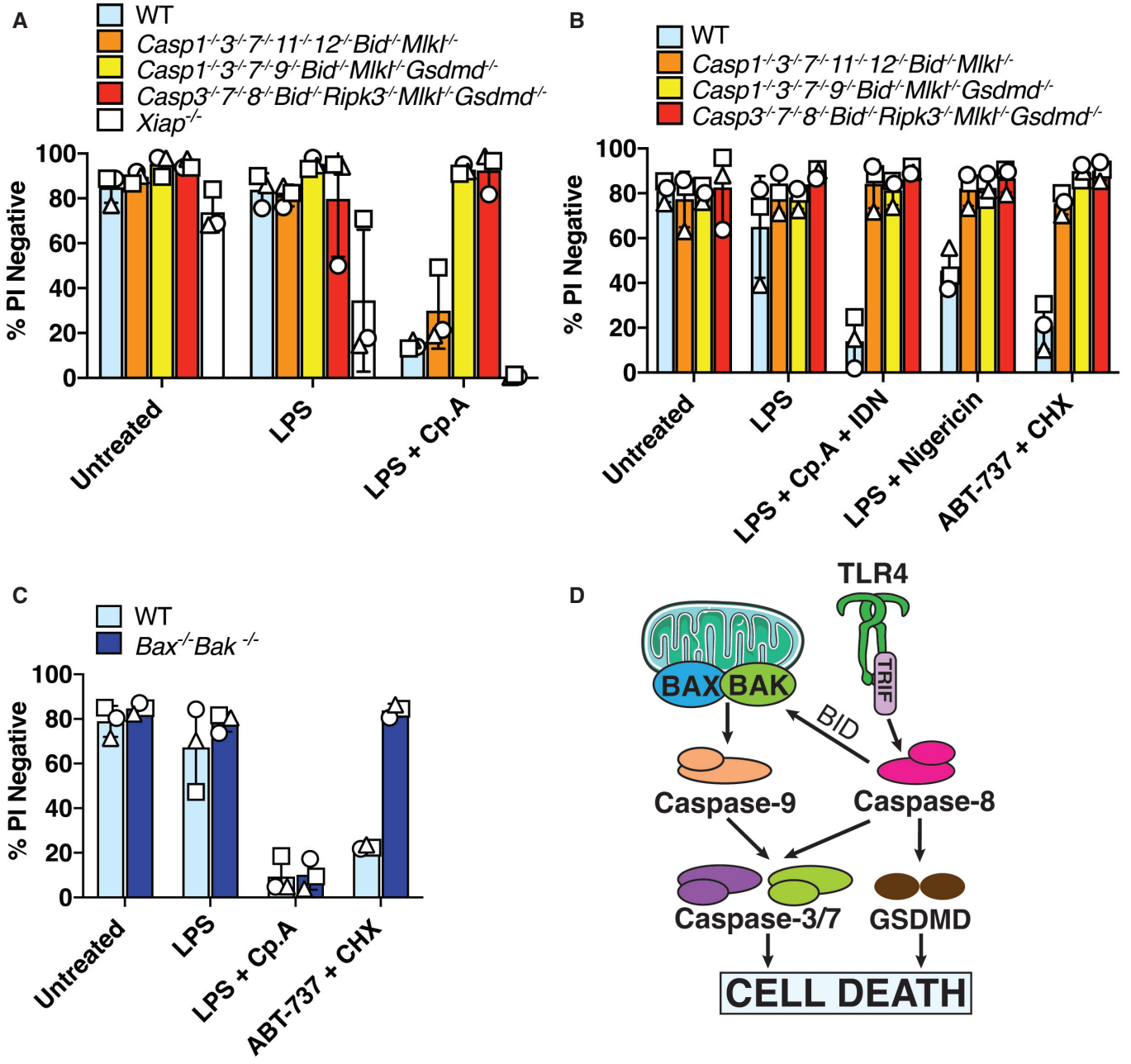

Figure 6. In the absence of the downstream apoptotic machinery, caspase-8-mediated cleavage and activation of GSDMD are required for cell death upon IAP inhibition.

A iBMDMs of the indicated genotypes were seeded at a density of 2 × 10^5 cells per well and were primed with 50 ng/ml LPS for 3 h then treated with Cp. A (2 μM) for 24 h. Cell viability was determined by PI staining and flow cytometry and measured as a proportion of PI-negative (live) cells. Data represent the mean of three independent experiments (symbols). Error bars are the mean ± SD.

B, C iBMDMs of the indicated genotypes seeded at a density of 2 × 10^5 cells per well were treated with ABT-737 (1 μM) and CHX (20 μg/ml) for 6 h, or LPS (50 ng/ml) and Cp. A (2 μM) and IDN-6556 (10 μM) for 24 h, or with LPS (50 ng/ml) for 3 h followed by nigericin (10 μM) for 1.5 h. Cell viability was determined by PI staining and flow cytometry and measured as a proportion of PI-negative (live) cells. Data represent the mean of three independent experiments (symbols). Error bars are the mean ± SD.

D Schematic model for how intrinsic and extrinsic cell death signalling are executed in macrophages.

Source data are available online for this figure.

having a key non-apoptotic transcriptional role in TLR-inflammasome priming (Allam *et al*, 2014), cells lacking caspase-8 (*Caspase-3*$^{-/-}$*7*$^{-/-}$*8*$^{-/-}$*Bid*$^{-/-}$*Ripk3*$^{-/-}$*Mlkl*$^{-/-}$*Gsdmd*$^{-/-}$ iBMDMs) displayed reduced LPS-induced NLRP3 and precursor IL-1β expression, and also exhibited decreased TNF secretion (Fig 7A and B; Appendix Fig S4).

Analysis of IL-1β activation responses in gene-targeted iBMDMs revealed that, as expected, iBMDMs lacking XIAP, or WT iBMDMs where XIAP was inhibited with Cp. A, secreted significant levels of IL-1β into the cell supernatants (Fig 7A and B). Notably, consistent with our hypothesis that, as a result of IAP deficiency, caspase-1, 3, 7, BID and GSDMD act redundantly to allow for IL-1β release downstream of caspase-8, only the combined absence of caspase-1, 3, −7, BID and GSDMD (i.e. *caspase-1$^{-/-}$3$^{-/-}$7$^{-/-}$9$^{-/-}$Bid$^{-/-}$Mlkl$^{-/-}$Gsdmd$^{-/-}$* iBMDMs) or caspase-8 (*Caspase-3$^{-/-}$7$^{-/-}$8$^{-/-}$Bid$^{-/-}$Ripk3$^{-/-}$Mlkl$^{-/-}$Gsdmd$^{-/-}$* iBMDMs) abrogated IL-1β egress (Fig 7A and B). In contrast, cells retaining caspase-8 and GSDMD (i.e. *Caspase-1$^{-/-}$3$^{-/-}$7$^{-/-}$11$^{-/-}$12$^{-/-}$Bid$^{-/-}$Mlkl$^{-/-}$*)

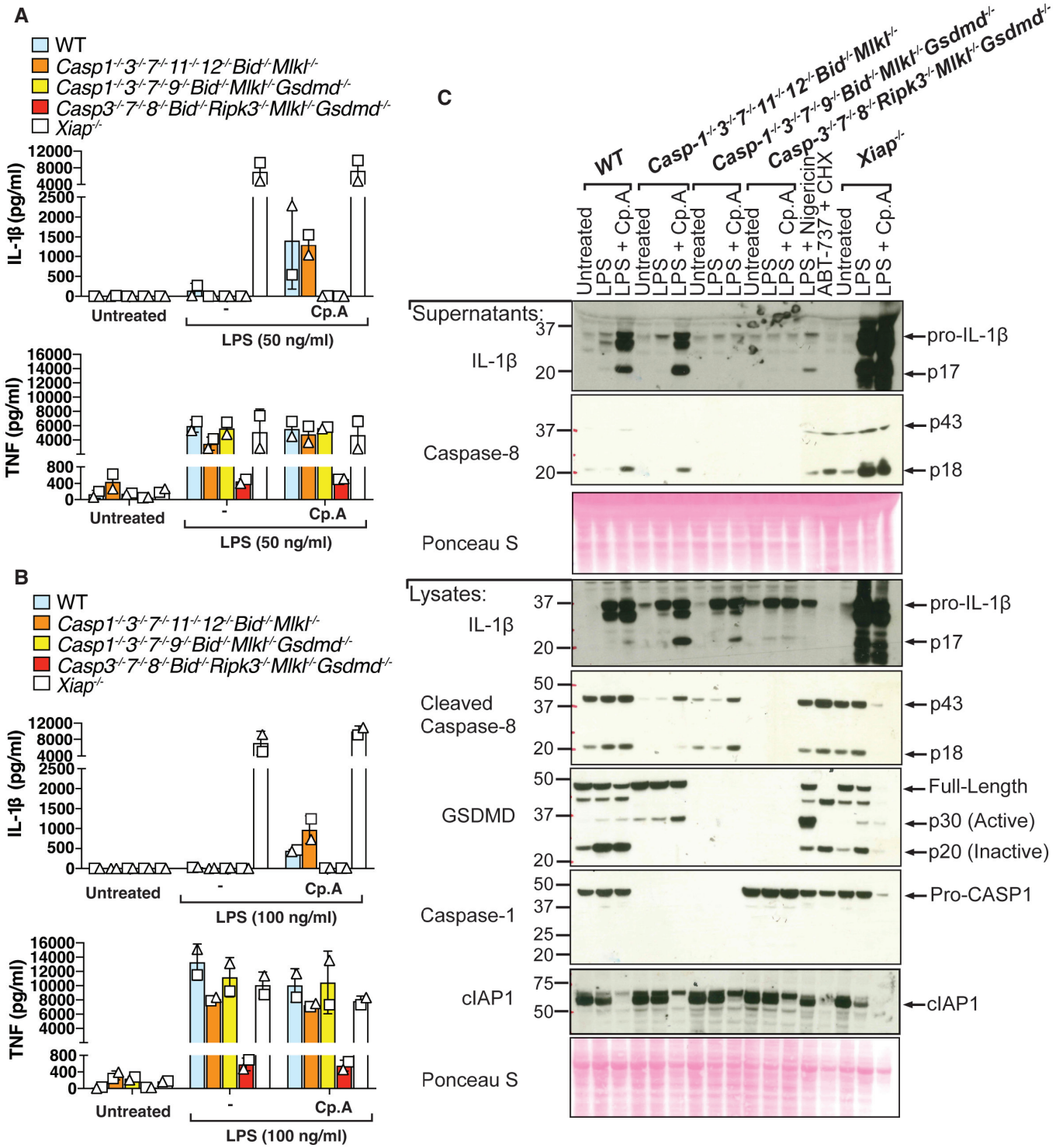

Figure 7.

Figure 7. In the absence of apoptotic and pyroptotic caspases, IAP loss triggers caspase-8-mediated processing of IL-1β and GSDMD to allow IL-1β activation and release.

A, B iBMDMs of the indicated genotypes were seeded at a density of 4 × 10^5 cells per well and primed with either 50 ng/ml (A) or 100 ng/ml (B) of LPS for 3 h then treated with Cp. A (2 μM) for 24 h. Cell supernatants were analysed by ELISA for levels of IL-1β and TNF, as indicated. Data represent the mean of two independent experiments, error bars are the mean ± SD.

C iBMDMs of the indicated genotypes were seeded at a density of 4 × 10^5 cells per well and primed with 100 ng/ml of LPS for 3 h then treated with Cp. A (2 μM) for 24 h. As control stimuli, WT iBMDMs were primed with LPS (100 ng/ml) for 3 h then treated with nigericin (10 μM) for 1.5 h or ABT-737 (1 μM) and CHX (20 μg/ml) for 6 h. Total cell lysates and supernatants were analysed by western blot. Ponceau staining depicts protein loading. Data representative of four independent experiments.

Source data are available online for this figure.

released levels of IL-1β comparable to WT iBMDMs (Fig 7A and B).

To ensure the GSDMD-dependent IL-1β release we observed by ELISA in the absence of caspase-1, caspase-3, caspase-7, caspase-11 and caspase-12 represented the active IL-1β p17 fragment, we next analysed cell lysates and cell supernatants by Western blot (noting that the IL-1β ELISA (R&D) can detect both precursor and mature forms of IL-1β (Conos *et al*, 2017)). Importantly, LPS priming and Cp. A treatment resulted in bioactive IL-1β release into the cell supernatant in *Caspase-1*$^{-/-}$*3*$^{-/-}$*7*$^{-/-}$*11*$^{-/-}$*12*$^{-/-}$*Bid*$^{-/-}$*Mlkl*$^{-/-}$ iBMDMs, akin to WT cells (Fig 7C). XIAP-deficient iBMDMs, as expected, also released large amounts of processed IL-1β upon treatment with LPS alone or in combination with Cp. A (Fig 7C). Critically, *Caspase-1*$^{-/-}$*3*$^{-/-}$*7*$^{-/-}$*9*$^{-/-}$*Bid*$^{-/-}$*Mlkl*$^{-/-}$*Gsdmd*$^{-/-}$ iBMDMs were completely deficient in Cp. A-mediated release of activated IL-1β, with the bioactive IL-1β p17 fragment only detectable in the cell lysate (Fig 7C). The cleavage of IL-1β in both cell lysates and supernatants was abrogated upon deletion of caspase-8 (*Caspase-3*$^{-/-}$*7*$^{-/-}$*8*$^{-/-}$*Bid*$^{-/-}$*Ripk3*$^{-/-}$*Mlkl*$^{-/-}$*Gsdmd*$^{-/-}$ iBMDMs) (Fig 7C), consistent with previous studies using primary BMDMs lacking RIPK3 and caspase-8 (Vince *et al*, 2012; Lawlor *et al*, 2015). The pore-forming p30 fragment of GSDMD was also moderately enriched upon IAP targeting in WT and *Caspase-1*$^{-/-}$*3*$^{-/-}$*7*$^{-/-}$*11*$^{-/-}$*12*$^{-/-}$*Bid*$^{-/-}$*Mlkl*$^{-/-}$ iBMDMs (Fig 7C), in line with caspase-8-mediated proteolysis of both IL-1β and GSDMD. Therefore, even in the absence of the downstream apoptotic machinery, caspase-8 can not only cleave IL-1β to its bioactive form but can also cleave GSDMD to trigger efficient cell death and promote IL-1β egress.

Discussion

Here we demonstrate that two patients with XIAP deficiency diagnosed with IBD display heightened markers of caspase-8 and GSDMD activity, in addition to increased IL-1β activation and release. Using IAP antagonist (Smac-mimetic) treatment, we further identify that the apoptotic machinery and GSDMD act redundantly to cause both cell death and IL-1β release upon the loss of IAP function. Caspase-3 and -7 cleavage of pannexin-1 were not required for triggering potassium ion efflux-induced NLRP3 inflammasome assembly downstream of caspase-8, unlike NLRP3 activation resulting from mitochondrial apoptosis. These findings delineate cell death and inflammatory pathways relevant to XIAP deficiency, and uncouple the downstream signalling events of intrinsic and extrinsic apoptosis that drive macrophage killing and NLRP3 inflammasome responses.

XIAP deficiency sensitises individuals to microbial-induced cell death and inflammatory-associated diseases, which are most commonly present as X-Linked HLH or CD. Our results indicate that pathogenic XIAP variants can allow for increased cell death and inflammatory responses in both the colonic mucosae and PBMCs and that this reflects heightened caspase-8, GSDMD and IL-1β activation. The intravenous administration of anakinra, a biologic IL-1 receptor antagonist, is an off-licence treatment used for secondary HLH and MAS and can reduce mortality (Bami *et al*, 2020; Eloseily *et al*, 2020; Maniscalco *et al*, 2020; Mehta *et al*, 2020). IL-1β can also mediate intestinal inflammation in mice and humans in certain conditions, such as IL-10 Receptor deficiency (Coccia *et al*, 2012; Shouval *et al*, 2016). Whether neutralisation of the elevated IL-1β activation observed in mice and humans lacking XIAP will be of wide-spread clinical utility in HLH or CD, beyond reported case studies (e.g. (Christiansen *et al*, 2016)), remains to be determined. In particular, the activation of the related inflammasome-associated cytokine, IL-18, by caspase-1 and/or − 8 is also heightened in HLH- and XIAP-deficient patients (Takada *et al*, 2001; Wada *et al*, 2014), and has been proposed as an additional therapeutic candidate in HLH, MAS and IBD (Monteleone *et al*, 1999; Kanai *et al*, 2001, 2003; Ludwiczek *et al*, 2005; Jarry *et al*, 2015; Mokry *et al*, 2019; Krei *et al*, 2021; Geerlinks *et al*, 2022).

An alternative to inhibiting IL-1β and/or IL-18 is to target the upstream intracellular machinery responsible for their activation. This may have the added benefit of inhibiting pathological cell death signalling, which we show contributes to both intracellular IL-1β activation and its egress into the extracellular milieu upon the loss of XIAP function. These findings are consistent with past research defining how distinct cell death pathways can operate to trigger inflammasome responses (Vince & Silke, 2016; Gaidt & Hornung, 2018). In the case of XIAP deficiency, our study identifies that two critical cell death initiators and effectors, caspase-8 and GSDMD, are activated in patient colonic mucosae and PBMCs. Previous research has shown that, upon IAP loss, caspase-8 is required for cell death and NLRP3-caspase-1 inflammasome assembly (Vince *et al*, 2012; Yabal *et al*, 2014; Lawlor *et al*, 2015, 2017; Knop *et al*, 2019). While the assumption has been that caspase-8-mediated macrophage killing represents the traditional extrinsic apoptotic pathway prevented by caspase-3 and -7 deletion (Lakhani *et al*, 2006), our findings demonstrate that apoptotic caspases and GSDMD can act redundantly in the context of IAP targeting. Evidence for this plasticity in cell death signalling has recently emerged during pathogen infections (Bedoui *et al*, 2020), and as our study now uncovers, the co-opting of more than one cell death modality also applies to autoinflammatory conditions.

We observed caspase-9 processing upon IAP inhibition; a hallmark of apoptosome formation downstream of BAX/BAK-mediated mitochondrial outer membrane permeabilization. Caspase-8 can contribute to BAX/BAK activation via its transcriptional roles or its cleavage of BID (Li *et al*, 1998; Simpson *et al*, 2022). Therefore, even though our genetic data show that BAX/BAK deficiency has no impact on LPS killing upon Cp. A treatment, and that the loss of BID did not impede cell death resulting from XIAP targeting, as expected (Jost *et al*, 2009), it remains possible that BAX/BAK act redundantly with caspase-8 triggering of caspase-1, −3, −7 and GSDMD. Caspase-1 has also been shown to contribute to caspase-3 and -7 activation in some situations (Sagulenko *et al*, 2017; de Vasconcelos *et al*, 2020). However, caspase-3 and -7 processing was not altered in caspase-1-deficient macrophages upon IAP antagonism, nor was cell death reduced upon caspase-1 inhibition alone, or even when combined with GSDMD and GSDME removal, indicating that any role caspase-1 plays is likely to be minor.

Our findings reveal important differences in both the execution of intrinsic and extrinsic cell death and in their triggering of the NLRP3 inflammasome. Unlike the rapid extrinsic caspase-8-driven cell death that can occur in the absence of caspase-3 and caspase-7, efficient BAX and BAK-mediated cell death was markedly reduced when caspase-3 and caspase-7 were deleted. Notably, in the context of BAX and BAK signalling we genetically proved, via the generation of pannexin-1-deficient and caspase cleavage resistant pannexin-1 mutant mice, that caspase-3 and caspase-7 can cause NLRP3 inflammasome assembly via their cleavage of pannexin-1, in agreement with previous findings (Vince *et al*, 2018; Chen *et al*, 2019). However, unlike previous research implicating pannexin-1 (Chen *et al*, 2019) or GSDMD (Donado *et al*, 2020) in caspase-8-driven NLRP3 activation, our data show that NLRP3 inflammasome assembly is not compromised by the individual loss of GSDMD or pannexin-1 in either IAP or TAK1 inhibited cells. Combined GSDMD and Pannexin-1 removal may suffice to block NLRP3 signalling upon caspase-8 activation, although this hypothesis remains to be experimentally tested.

Overall, our findings show that it will be important to examine in relevant pre-clinical HLH and IBD models whether efficient therapeutic responses can be achieved by inhibiting IL-1β and/or IL-18. It remains of outstanding interest whether co-targeting the key apoptotic and pyroptotic machinery, identified herein as executing the inflammatory cell death resulting from XIAP loss, could also be therapeutically inhibited in HLH and IBD.

Materials and Methods

Patients

The Medical Ethics Committee of Guangzhou Women and Children's Medical Centre approved the study procedures (ID: 2017021504). The implementations were in concordance with the International Ethical Guidelines for Research Involving Human Subjects as stated in the Helsinki Declaration. Informed written consent was obtained from the legal guardians of all participants. Patients had baseline demographics recorded, including clinical features, disease durations, family histories, extra-intestinal diseases, and laboratory test results. All patients underwent routine examinations prior to colonoscopy to exclude bacterial, viral, and parasitic infections, as well as tuberculosis and malignancies.

Patient sequencing

Whole Exome sequencing and sanger sequencing was performed at the Beijing Genomic Institute (BGI).

Immunofluorescence

Immunofluorescent staining was performed as previously described (Huang *et al*, 2019). Briefly, paraffin-embedded sections of colonic biopsies were processed as reported (Zhang *et al*, 2018). Sections were deparaffinised, incubated with blocking buffer (PBS with 5% normal donkey or goat serum and 0.3% Triton X-100) at room temperature for 1 h and stained with primary antibodies overnight in a wet chamber at 4°C in the dark. Sections were then washed with PBS, incubated with secondary antibodies for 1 h at room temperature in the dark, and mounted with VECTASHIELD Antifade Mounting Medium with DAPI (H-1200, Vector Laboratories, CA, USA) for nuclear staining. Immunofluorescent images were acquired with a Leica TCS SP8 Inverted Fluorescence Microscope (Leica Microsystems) using a 20 × 0.75 dry objective lens. Post-acquisition processing (brightness, opacity, contrast and colour balance) was applied to the entire image and accurately reflected the results of the original image. For each single colonic mucosae image, the amount of cleaved GSDMD or caspase-8 staining per square millimetre was divided by the area of DAPI staining. Images were analysed using Leica X image analysis software (Leica, Hamburg, Germany) and ImageJ software (National Institutes of Health, MD, USA). The primary and secondary antibodies used for immunostaining were cleaved GSDMD (Cell Signalling: 36425) and cleaved Caspase-8 (Affinity: AF5267), and the secondary antibody used was Alexa Fluor™ 594 goat anti-rabbit (Thermo Fisher: A-11012).

Colonoscopies

Colonoscopies were performed at the Guangzhou Women and Children's Medical Centre. The endoscopic activity of colonic tissue was determined by experienced gastrointestinal (GI) endoscopists using the Modified Mayo Endoscopic Score (MES) criteria.

Isolation, culture and stimulation of human peripheral blood mononuclear cells

PBMCs from healthy donors and XIAP-deficient patients were isolated by Ficoll density gradients and dispensed in 96-well plates at a density of 2–3 × 10^5 cells/well in 200 µl of R10 media (RPMI 1640, 10% foetal bovine serum (FBS), 100 units/ml penicillin and 100 mg/mL streptomycin), and incubated at 37°C in 5% CO_2. PBMCs were subsequently stimulated with LPS (500 ng/ml (InvivoGen), 24 h) or with MDP (10 µg/ml (InvivoGen), 24 h) and cell lysates and supernatants taken for western blot and ELISA analysis, respectively.

Mice

WT C57BL/6 mice and gene-targeted animals were bred at the Walter and Eliza Hall Institute of Medical Research (WEHI, Parkville,

Australia) and/or obtained from WEHI animal supplies (Kew, Australia). The generation and characterisation of the pannexin-1 and pannexin-1 non-cleavable (D375A and D378A) mice will be described elsewhere. *Casp1*$^{-/-}$ (Kuida *et al*, 1995) and *Nlrp3*$^{-/-}$ (Martinon *et al*, 2006) mice generated on a C57BL/6J background, and *Gsdmd*$^{-/-}$ (Kayagaki *et al*, 2015a), *Gsdme*$^{-/-}$ (kindly provided by Genentech), and *Gsdmd*$^{-/-}$*Gsdme*$^{-/-}$ (bred in-house) mice generated on a C57BL/6N background, were housed under specific pathogen-free conditions at WEHI, Australia. Animal rooms are maintained at approximately 21°C ± 3°C at 40–70% humidity with a timed 14/10 light-dark cycle. All procedures were approved by the WEHI Animal Ethics Committee, Australia (Ethics 2020.038 and 2019.034). None of the mice used in our experiments had been previously used for other procedures. The animals presented with a healthy status and were selected independently of their sex for generating macrophages. Female and male mice were 7–14 weeks old at the time of experimentation and their genotype was not blinded.

Cell culture

To generate macrophages, bone marrow cells were flushed from the femora and tibiae of male or female mice aged 6–14 weeks. Bone merrow cells were cultured in Dulbecco's Modified Eagle Medium (DMEM) supplemented with 10% Foetal Bovine Serum (FBS), 100 U/ml Penicillin, 100 μg/ml Streptomycin, and 20% L929 conditioned supernatant (containing Macrophage Colony-Stimulating Factor [M-CSF] on 15-centimetre Petri dishes for 7 days at 37°C in 10% CO_2). Where indicated, BMDMs were immortalised using Cre-J2 virus (Rapp *et al*, 1985) and CRISPR/Cas9 gene targeting of iBMDMs was performed as described previously (Doerflinger *et al*, 2020). iBMDMs were cultured in DMEM 10% FBS supplemented with 100 U/ml Penicillin and 100 mg/ml Streptomycin at 37°C in 10% CO_2. MEFs derived from WT and caspase-3 and caspase-7-deficient mice, as well as HEK293 T cells, were cultured in identical conditions to iBMDMs. Cell lines were routinely tested for mycoplasma but were not authenticated by DNA profiling.

Cell stimulations

For stimulations, macrophages (BMDMs and iBMDMs) were plated out on TC-treated (for western blotting) or non-TC treated (for cell death analysis) 24 well tissue culture plates at 500,000 cells/well in 0.5 ml of media and were allowed to adhere to the plate. Macrophages were then treated where indicated with LPS (50–100 ng/ml, InvivoGen; tlrl-3pelps). Where multiple time points were used for analysis, TLR stimulations were performed in a reverse-time-course fashion so that all cells were harvested at the same time. In this instance, single treatment controls were added for the longest time point measured. LPS, nigericin (10 μM, Sigma; N7143), Smac-mimetics Cp. A, 030, 031, 455, 711, 851 and 883 (500 nM - 2 μM, kindly provided by TetraLogic Pharmaceuticals), TAK1 inhibitor (5Z)-7-Oxozeaenol (125–500 nM, Tocris; 3604), MCC950 (1–5 μM, kindly provided by A. Roberson and M. Cooper, University of Queensland, Australia), ABT-737 (1 μM, Active Biochem; A-6044) and cycloheximide (20 μg/ml, Sigma; C7698) treatments were performed as indicated in the relevant figure legends. Experiments were repeated independently (2–4 times on average) to ascertain reproducibility and the number of repeats performed for data presented in each figure panel is stated in the figure legends. In cases where variability was observed more repeats were generated unless there was an obvious technical error.

Western blotting

Cells or cell-free supernatants were lysed in SDS (2%) lysis buffer with β-mercaptoethanol (143 mM). Reduced and denatured total cell lysates and supernatants were loaded onto 20-well 4–12% gradient gels (Invitrogen) and separated by electrophoresis at 120 V for 2 h. Proteins were transferred onto nitrocellulose membranes (Amersham) through electrophoretic transfer at 110 V for 90–110 min at 4°C. Protein loading was evaluated using Ponceau-S stain before membrane-blocking in Tris-buffered saline containing 0.1% Tween (TBS-T) and 5% w/v skim milk (Devondale) for 1 h at 4°C. Blocked membranes were probed overnight with primary antibodies. After primary antibody incubation membranes were washed five times in TBS-T for 1 h before the application of species-appropriate secondary antibodies conjugated to horse radish peroxidase for 1 h at room temperature. After secondary antibody incubation membranes were washed 4–10 times for 1 h in TBS-T. Blots were developed using ECL (Amersham or Millipore) and film on a Kodak X-OMAT film processor or by the ChemiDoc Touch Imaging System (Bio-Rad) and Image Lab software. Primary antibodies were diluted in TBS-T containing 5% w/v BSA and 0.05% Sodium Azide or PBS-T containing 5% w/v Skim Milk and 0.05% Sodium Azide. All secondary antibodies were diluted in TBS-T containing 5% w/v skim milk.

Antibodies

For mouse cell analysis membranes were probed with primary antibodies overnight at 4°C (all diluted 1:1,000 in TBS-T containing 5% w/v BSA or PBS-T containing 5% w/v Skim Milk, unless stated otherwise). The antibodies used were β-actin (Sigma; A-1798), caspase-1 (Adipogen; AG-20B-0042-C100), cleaved caspase-8 Asp387 (Cell Signalling; 9429, 8592), caspase-9 (Cell Signalling; 9509), caspase-3 (Cell Signalling; 9662), caspase-9 (Cell Signalling; 9508), pro-caspase-8 (in-house, 3B10), caspase-7 (Cell Signalling; 9492), GSDMD (Abcam; ab209845), GSDME (Abcam; ab215191), IL-1β (R&D; AF-401-NA), MLKL (in-house; Murphy *et al*, 2013; 3H1, available as MABC604 from Merck Millipore), XIAP (MBL; M044-3), pannexin-1 (Cell Signalling; (D9M1C) 91137), ASC (Santa Cruz Biotech; sc-22514), RIPK3 (Axxora; PSC-2283-c100), BID (2D1; in-house; Kaufmann *et al*, 2007), caspase-6 (Cell Signalling; 9672), NLRP3 (Adipogen; AG-20B-0014-C100), MCL-1 (Cell Signalling; 5453) and FLAG (Sigma-Aldrich; F3165). For human cell western blotting, the antibodies used were XIAP (Cell Signalling: 2042), caspase-8 (Cell Signalling: 9746), cleaved GSDMD (Cell Signalling: 36425) and cleaved IL-1β (Cell Signalling: 83186). Relevant horseradish peroxidase-conjugated secondary antibodies (Jaxon laboratories) were diluted 1:10,000 in 5% skimmed milk in TBS-T applied for 1 h at room temperature.

Cell viability assays

Cell viability was determined by PI staining and flow cytometry. At the end point of experiments, cell supernatants were collected and

transferred into FACS tubes. Adherent cells on non-tissue culture treated plates were detached using 5 mM EDTA pH 8.0 in PBS (3–5 min incubation at room temperature). Cells were then harvested and transferred to the FACS tube containing their corresponding supernatant. PI was added such that the final concentration was 1–5 μg/ml. Cells were analysed using an LSRII cytometer (Becton Dickinson, NJ) and WEASEL version 2.7 software (Frank Battye) or FlowJo software. PI exclusion analysis for each sample was performed with 10,000 single-cell events.

IncuCyte live cell imaging analysis

BMDMs were seeded in triplicate at a density of 7.5×10^4 cells per well into 96-well plates in DMEM 10% FCS supplemented with 20% L929-conditioned supernatant. 1:2,000 dilution of SYTOX Green (Sartorius 4633) and 1:1,000 of SPY620-DNA (Spirochrome SC401) dyes were added to medium 1 h before cell treatment and image acquisition. Plates were analysed in an IncuCyte S3 System (Essen Biosciences) using a 10-× objective over time using red, green and brightfield channels, and images were taken once every 30 min for 14 h. The percentage of cell death was calculated as the number of SYTOX Green positive cells versus total SPY620-DNA positive cells. For quantification, three views were taken per well and the mean cell counts of these views were taken and plotted. Data presented are representative of three independent experiments.

Cytokine analysis

Cell supernatants were analysed by ELISA for murine TNF (Invitrogen, 88-7324-88), murine IL-1β (R&D, DY401) or human IL-1β, TNF and IL-6 (Thermo Fischer) levels according to the manufacturer's instructions. BMDM-derived supernatants were diluted 1:2 in sterile PBS for IL-1β quantification, and 1:8 for TNF quantification. iBMDM-derived supernatants were left undiluted for IL-1β analysis or diluted 1:4 for TNF measurements. All values obtained from ELISA plates were multiplied by their respective dilution factor.

ASC cross-linking

BMDMs were seeded into tissue-culture-treated 6-well plates at a density of 2×10^6 cells per well. After priming with 100 ng/ml LPS for 2–3 h, the culture medium was removed and replaced with opti-MEM. Cells were then treated with the indicated compounds (see figure legends). At the end point of experiments, cell supernatants were collected. Adherent cells were washed once with ice-cold PBS before adding 225 μl ice-cold MilliQ water containing an EDTA-free protease inhibitor cocktail (Roche). Cells were then freeze-thawed at −80°C to cause lysis. Lysates were adjusted by the addition of 25 μl of 10× PBS, were spun at 6,000 *g* at 4°C for 15 min, and lysate pellets resuspended in 200 μl of PBS. To cross-link these pellets, 2 mM (final concentration) of disuccinimidyl suberate was added to each tube, and the samples were left to incubate at 37°C for 45 min with occasional agitation every 5–10 min. Cross-linked pellets were spun at 21,000 *g* for 20 min at 4°C. Supernatants were discarded, and pellets were resuspended in 100 μl of lysis buffer for western blot analysis.

293 T GSDMD cleavage assays

10 μg of FLAG-GSDMD (Addgene #80950 (Liu *et al*, 2016)) was transfected into a 10 cm plate of (~ 80% confluent) 293 T cells. After 24 h cells were re-plated into 24 well tissue culture plates and transfected with 0.5 μg of caspase-1 or caspase-8 cDNA as indicated in EV Fig 5. The following day total cell lysates were generated and analysed by western blot.

Data availability

This study includes no data deposited in external repositories.

Expanded View for this article is available online.

Acknowledgements

We gratefully thank Dr Aysha Al-Ani for advice and acknowledge grant support from the National Natural Science Foundation of China (92042303, 82125015 to Y.Z.; 81901665 to M.L.) and National Health and Medical Research Council (NHMRC) of Australia: project grants (1145788 to J.E.V., K.E.L.; 1101405 to J.E.V.; 1162765 to K.E.L.; 1143105 to M.J.H.), ideas grants (1183070 to J.E.V.; 1181089 to K.E.L.), investigator grants (1172929 to J.M.M; 1175011 to M.P.; 2008692 to J.E.V.), fellowships (1141466 to J.E.V.; 1144014 to S.A.C.) and the Leukaemia and Lymphoma Society (LLS SCOR 7015-18 to M.J.H.). K.E.L. is an Australian Research Council (ARC) Future Fellow (FT190100266). M.J.H. is a NHMRC Senior Research Fellow (1156095). The contents of the published materials are solely the responsibility of the individual authors and do not reflect the views of the NHMRC. D.S.S. is supported by a philanthropic PhD scholarship from the Walter and Eliza Hall Institute of Medical Research. This work was also supported by operational infrastructure grants through the Australian Government Independent Research Institute Infrastructure Support Scheme (9000719) and the Victorian State Government Operational Infrastructure Support, Australia.

Author contributions

Sebastian A Hughes: Data curation; formal analysis; investigation; methodology; writing—original draft; writing—review and editing. **Meng Lin:** Data curation; formal analysis; investigation; methodology; funding acquisition. **Ashley Weir:** Data curation; formal analysis; investigation. **Bing Huang:** Investigation. **Liya Xiong:** Resources; project administration. **Ngee Kiat Chua:** Formal analysis; investigation. **Jiyi Pang:** Formal analysis; investigation. **Jascinta P Santavanond:** Resources; investigation. **Rochelle Tixeira:** Resources; investigation. **Marcel Doerflinger:** Resources. **Yexuan Deng:** Resources; investigation. **Chien-Hsiung Yu:** Investigation. **Natasha Silke:** Investigation. **Stephanie A Conos:** Investigation. **Daniel Frank:** Investigation. **Daniel S Simpson:** Investigation; writing—review and editing. **James M Murphy:** Resources; supervision; funding acquisition; writing—review and editing. **Kate E Lawlor:** Supervision; investigation; writing—review and editing; funding acquisition. **Jaclyn S Pearson:** Supervision; investigation; writing—review and editing. **John Silke:** Resources. **Marc Pellegrini:** Resources; funding acquisition. **Marco Herold:** Resources; supervision; funding acquisition. **Ivan KH Poon:** Resources; supervision. **Seth L Masters:** Supervision. **Mingsong Li:** Resources. **Qing Tang:** Investigation. **Yuxia Zhang:** Formal analysis; supervision; funding acquisition; investigation; methodology; writing—original draft; writing—review and editing. **Maryam Rashidi:** Formal analysis; supervision; investigation; writing—review and editing. **Lanlan Geng:** Conceptualization; resources; supervision; project administration. **James E Vince:**

Conceptualization; resources; formal analysis; supervision; funding acquisition; investigation; methodology; writing—original draft; project administration; writing—review and editing.

Disclosure and competing interests

The authors declare that they have no conflict of interest.

References

Aglietti RA, Estevez A, Gupta A, Ramirez MG, Liu PS, Kayagaki N, Ciferri C, Dixit VM, Dueber EC (2016) GsdmD p30 elicited by caspase-11 during pyroptosis forms pores in membranes. *Proc Natl Acad Sci USA* 113: 7858 – 7863

Aguilar C, Latour S (2015) X-linked inhibitor of apoptosis protein deficiency: more than an X-linked lymphoproliferative syndrome. *J Clin Immunol* 35: 331 – 338

Aguilar C, Lenoir C, Lambert N, Begue B, Brousse N, Canioni D, Berrebi D, Roy M, Gerart S, Chapel H *et al* (2014) Characterization of Crohn disease in X-linked inhibitor of apoptosis-deficient male patients and female symptomatic carriers. *J Allergy Clin Immunol* 134: 1131 – 1141.e39

Allam R, Lawlor KE, Yu EC, Mildenhall AL, Moujalled DM, Lewis RS, Ke F, Mason KD, White MJ, Stacey KJ *et al* (2014) Mitochondrial apoptosis is dispensable for NLRP3 inflammasome activation but non-apoptotic caspase-8 is required for inflammasome priming. *EMBO Rep* 15: 982 – 990

Alvarez-Diaz S, Dillon CP, Lalaoui N, Tanzer MC, Rodriguez DA, Lin A, Lebois M, Hakem R, Josefsson EC, O'Reilly LA *et al* (2016) The Pseudokinase MLKL and the kinase RIPK3 have distinct roles in autoimmune disease caused by loss of death-receptor-induced apoptosis. *Immunity* 45: 513 – 526

Amininejad L, Charloteaux B, Theatre E, Liefferinckx C, Dmitrieva J, Hayard P, Muls V, Maisin JM, Schapira M, Ghislain JM *et al* (2018) Analysis of genes associated with monogenic primary immunodeficiency identifies rare variants in XIAP in patients with Crohn's disease. *Gastroenterology* 154: 2165 – 2177

Arico M, Janka G, Fischer A, Henter JI, Blanche S, Elinder G, Martinetti M, Rusca MP (1996) Hemophagocytic lymphohistiocytosis. Report of 122 children from the international registry. FHL study Group of the Histiocyte Society. *Leukemia* 10: 197 – 203

Aubrey BJ, Kelly GL, Kueh AJ, Brennan MS, O'Connor L, Milla L, Wilcox S, Tai L, Strasser A, Herold MJ (2015) An inducible lentiviral guide RNA platform enables the identification of tumor-essential genes and tumor-promoting mutations in vivo. *Cell Rep* 10: 1422 – 1432

Baker PJ, Boucher D, Bierschenk D, Tebartz C, Whitney PG, D'Silva DB, Tanzer MC, Monteleone M, Robertson AA, Cooper MA *et al* (2015) NLRP3 inflammasome activation downstream of cytoplasmic LPS recognition by both caspase-4 and caspase-5. *Eur J Immunol* 45: 2918 – 2926

Bami S, Vagrecha A, Soberman D, Badawi M, Cannone D, Lipton JM, Cron RQ, Levy CF (2020) The use of anakinra in the treatment of secondary hemophagocytic lymphohistiocytosis. *Pediatr Blood Cancer* 67: e28581

Bedoui S, Herold MJ, Strasser A (2020) Emerging connectivity of programmed cell death pathways and its physiological implications. *Nat Rev Mol Cell Biol* 21: 678 – 695

Canna SW, Girard C, Malle L, de Jesus A, Romberg N, Kelsen J, Surrey LF, Russo P, Sleight A, Schiffrin E *et al* (2017) Life-threatening NLRC4-associated hyperinflammation successfully treated with IL-18 inhibition. *J Allergy Clin Immunol* 139: 1698 – 1701

Chang I, Park S, Lee HJ, Kim I, Park S, Ahn MK, Lee J, Kang M, Baek IJ, Sung YH *et al* (2021) Interpretation of XIAP variants of uncertain significance in Paediatric patients with refractory Crohn's disease. *J Crohns Colitis* 15: 1291 – 1304

Chauhan D, Bartok E, Gaidt MM, Bock FJ, Herrmann J, Seeger JM, Broz P, Beckmann R, Kashkar H, Tait SWG *et al* (2018) BAX/BAK-induced apoptosis results in Caspase-8-dependent IL-1beta maturation in macrophages. *Cell Rep* 25: 2354 – 2368.e55

Chen KW, Demarco B, Heilig R, Shkarina K, Boettcher A, Farady CJ, Pelczar P, Broz P (2019) Extrinsic and intrinsic apoptosis activate pannexin-1 to drive NLRP3 inflammasome assembly. *EMBO J* 38: e101638

Christiansen M, Ammann S, Speckmann C, Mogensen TH (2016) XIAP deficiency and MEFV variants resulting in an autoinflammatory lymphoproliferative syndrome. *BMJ Case Rep* 2016: bcr2016216922

Coccia M, Harrison OJ, Schiering C, Asquith MJ, Becher B, Powrie F, Maloy KJ (2012) IL-1beta mediates chronic intestinal inflammation by promoting the accumulation of IL-17A secreting innate lymphoid cells and CD4(+) Th17 cells. *J Exp Med* 209: 1595 – 1609

Coll RC, Robertson AA, Chae JJ, Higgins SC, Munoz-Planillo R, Inserra MC, Vetter I, Dungan LS, Monks BG, Stutz A *et al* (2015) A small-molecule inhibitor of the NLRP3 inflammasome for the treatment of inflammatory diseases. *Nat Med* 21: 248 – 255

Condon SM, Mitsuuchi Y, Deng Y, Laporte MG, Rippin SR, Haimowitz T, Alexander MD, Kumar PT, Hendi MS, Lee YH *et al* (2014) Birinapant, a Smac-mimetic with improved tolerability for the treatment of solid tumors and hematological malignancies. *J Med Chem* 57: 3666 – 3677

Conos SA, Chen KW, De Nardo D, Hara H, Whitehead L, Nunez G, Masters SL, Murphy JM, Schroder K, Vaux DL *et al* (2017) Active MLKL triggers the NLRP3 inflammasome in a cell-intrinsic manner. *Proc Natl Acad Sci U S A* 114: E961 – E969

Crayne CB, Albeituni S, Nichols KE, Cron RQ (2019) The immunology of macrophage activation syndrome. *Front Immunol* 10: 119

Damgaard RB, Nachbur U, Yabal M, Wong WW, Fiil BK, Kastirr M, Rieser E, Rickard JA, Bankovacki A, Peschel C *et al* (2012) The ubiquitin ligase XIAP recruits LUBAC for NOD2 signaling in inflammation and innate immunity. *Mol Cell* 46: 746 – 758

Demarco B, Grayczyk JP, Bjanes E, Le Roy D, Tonnus W, Assenmacher CA, Radaelli E, Fettrelet T, Mack V, Linkermann A *et al* (2020) Caspase-8-dependent gasdermin D cleavage promotes antimicrobial defense but confers susceptibility to TNF-induced lethality. *Sci Adv* 6: eabc3465

Doerflinger M, Deng Y, Whitney P, Salvamoser R, Engel S, Kueh AJ, Tai L, Bachem A, Gressier E, Geoghegan ND *et al* (2020) Flexible usage and interconnectivity of diverse cell death pathways protect against intracellular infection. *Immunity* 53: 533 – 547.e37

Donado CA, Cao AB, Simmons DP, Croker BA, Brennan PJ, Brenner MB (2020) A two-cell model for IL-1beta release mediated by death-receptor signaling. *Cell Rep* 31: 107466

Du C, Fang M, Li Y, Li L, Wang X (2000) Smac, a mitochondrial protein that promotes cytochrome c-dependent caspase activation by eliminating IAP inhibition. *Cell* 102: 33 – 42

Duckett CS, Nava VE, Gedrich RW, Clem RJ, Van Dongen JL, Gilfillan MC, Shiels H, Hardwick JM, Thompson CB (1996) A conserved family of cellular genes related to the baculovirus iap gene and encoding apoptosis inhibitors. *EMBO J* 15: 2685 – 2694

Eloseily EM, Weiser P, Crayne CB, Haines H, Mannion ML, Stoll ML, Beukelman T, Atkinson TP, Cron RQ (2020) Benefit of anakinra in treating pediatric secondary hemophagocytic Lymphohistiocytosis. *Arthritis & Rheumatol* 72: 326 – 334

Gaidt MM, Hornung V (2016) Pore formation by GSDMD is the effector mechanism of pyroptosis. *EMBO J* 35: 2167 – 2169

Gaidt MM, Hornung V (2018) The NLRP3 inflammasome renders cell death pro-inflammatory. *J Mol Biol* 430: 133 – 141

Gaidt MM, Ebert TS, Chauhan D, Schmidt T, Schmid-Burgk JL, Rapino F, Robertson AA, Cooper MA, Graf T, Hornung V (2016) Human monocytes engage an alternative inflammasome pathway. *Immunity* 44: 833 – 846

Geerlinks AV, Dvorak AM, Jordan MB, Schiffrin EJ, Behrens EM, Marsh R (2022) A case of XIAP deficiency successfully managed with Tadekinig Alfa (rhIL-18BP). *J Clin Immunol* 42: 901 – 903

Huang B, Chen Z, Geng L, Wang J, Liang H, Cao Y, Chen H, Huang W, Su M, Wang H *et al* (2019) Mucosal profiling of pediatric-onset colitis and IBD reveals common Pathogenics and therapeutic pathways. *Cell* 179: 1160 – 1176.e24

Janka GE (2012) Familial and acquired hemophagocytic lymphohistiocytosis. *Annu Rev Med* 63: 233 – 246

Jarry A, Bossard C, Droy-Dupre L, Volteau C, Bourreille A, Meurette G, Mosnier JF, Laboisse CL (2015) Heterogeneity of subordination of the IL-18/IFN-gamma axis to caspase-1 among patients with Crohn's disease. *Lab Invest* 95: 1207 – 1217

Jones JD, Vance RE, Dangl JL (2016) Intracellular innate immune surveillance devices in plants and animals. *Science* 354: aaf6395

Jost PJ, Grabow S, Gray D, McKenzie MD, Nachbur U, Huang DC, Bouillet P, Thomas HE, Borner C, Silke J *et al* (2009) XIAP discriminates between type I and type II FAS-induced apoptosis. *Nature* 460: 1035 – 1039

Kanai T, Watanabe M, Okazawa A, Sato T, Yamazaki M, Okamoto S, Ishii H, Totsuka T, Iiyama R, Okamoto R *et al* (2001) Macrophage-derived IL-18-mediated intestinal inflammation in the murine model of Crohn's disease. *Gastroenterology* 121: 875 – 888

Kanai T, Uraushihara K, Totsuka T, Okazawa A, Hibi T, Oshima S, Miyata T, Nakamura T, Watanabe M (2003) Macrophage-derived IL-18 targeting for the treatment of Crohn's disease. *Curr Drug Targets Inflamm Allergy* 2: 131 – 136

Kaufmann T, Tai L, Ekert PG, Huang DC, Norris F, Lindemann RK, Johnstone RW, Dixit VM, Strasser A (2007) The BH3-only protein bid is dispensable for DNA damage- and replicative stress-induced apoptosis or cell-cycle arrest. *Cell* 129: 423 – 433

Kayagaki N, Stowe IB, Lee B, O'Rourke KM, Warming S, Cuellar T, Haley B, Roose-Girma M, Phung Q, Liu PS *et al* (2015a) Caspase-11 cleaves gasdermin D for non-canonical inflammasome signaling. *Nature* 526: 666 – 671

Kayagaki N, Stowe IB, Lee BL, O'Rourke K, Anderson K, Warming S, Cuellar T, Haley B, Roose-Girma M, Phung QT *et al* (2015b) Caspase-11 cleaves gasdermin D for non-canonical inflammasome signalling. *Nature* 526: 666 – 671

Kayagaki N, Kornfeld OS, Lee BL, Stowe IB, O'Rourke K, Li Q, Sandoval W, Yan D, Kang J, Xu M *et al* (2021) NINJ1 mediates plasma membrane rupture during lytic cell death. *Nature* 591: 131 – 136

Knop J, Spilgies LM, Rufli S, Reinhart R, Vasilikos L, Yabal M, Owsley E, Jost PJ, Marsh RA, Wajant H *et al* (2019) TNFR2 induced priming of the inflammasome leads to a RIPK1-dependent cell death in the absence of XIAP. *Cell Death Dis* 10: 700

Krei JM, Moller HJ, Larsen JB (2021) The role of interleukin-18 in the diagnosis and monitoring of hemophagocytic lymphohistiocytosis/macrophage activation syndrome - a systematic review. *Clin Exp Immunol* 203: 174 – 182

Krieg A, Correa RG, Garrison JB, Le Negrate G, Welsh K, Huang Z, Knoefel WT, Reed JC (2009) XIAP mediates NOD signaling via interaction with RIP2. *Proc Natl Acad Sci U S A* 106: 14524 – 14529

Kuida K, Lippke JA, Ku G, Harding MW, Livingston DJ, Su MS, Flavell RA (1995) Altered cytokine export and apoptosis in mice deficient in interleukin-1 beta converting enzyme. *Science* 267: 2000 – 2003

Lakhani SA, Masud A, Kuida K, Porter GA Jr, Booth CJ, Mehal WZ, Inayat I, Flavell RA (2006) Caspases 3 and 7: key mediators of mitochondrial events of apoptosis. *Science* 311: 847 – 851

Lawlor KE, Khan N, Mildenhall A, Gerlic M, Croker BA, D'Cruz AA, Hall C, Kaur Spall S, Anderton H, Masters SL *et al* (2015) RIPK3 promotes cell death and NLRP3 inflammasome activation in the absence of MLKL. *Nat Commun* 6: 6282

Lawlor KE, Feltham R, Yabal M, Conos SA, Chen KW, Ziehe S, Grass C, Zhan Y, Nguyen TA, Hall C *et al* (2017) XIAP loss triggers RIPK3- and Caspase-8-driven IL-1beta activation and cell death as a consequence of TLR-MyD88-induced cIAP1-TRAF2 degradation. *Cell Rep* 20: 668 – 682

Li H, Zhu H, Xu CJ, Yuan J (1998) Cleavage of BID by caspase 8 mediates the mitochondrial damage in the Fas pathway of apoptosis. *Cell* 94: 491 – 501

Liston P, Roy N, Tamai K, Lefebvre C, Baird S, Cherton-Horvat G, Farahani R, McLean M, Ikeda JE, MacKenzie A *et al* (1996) Suppression of apoptosis in mammalian cells by NAIP and a related family of IAP genes. *Nature* 379: 349 – 353

Liu X, Zhang Z, Ruan J, Pan Y, Magupalli VG, Wu H, Lieberman J (2016) Inflammasome-activated gasdermin D causes pyroptosis by forming membrane pores. *Nature* 535: 153 – 158

Lluis JM, Nachbur U, Cook WD, Gentle IE, Moujalled D, Moulin M, Wong WW, Khan N, Chau D, Callus BA *et al* (2010) TAK1 is required for survival of mouse fibroblasts treated with TRAIL, and does so by NF-kappaB dependent induction of cFLIPL. *PLoS One* 5: e8620

Ludwiczek O, Kaser A, Novick D, Dinarello CA, Rubinstein M, Tilg H (2005) Elevated systemic levels of free interleukin-18 (IL-18) in patients with Crohn's disease. *Eur Cytokine Netw* 16: 27 – 33

Maelfait J, Vercammen E, Janssens S, Schotte P, Haegman M, Magez S, Beyaert R (2008) Stimulation of toll-like receptor 3 and 4 induces interleukin-1beta maturation by caspase-8. *J Exp Med* 205: 1967 – 1973

Mandal P, Feng Y, Lyons JD, Berger SB, Otani S, DeLaney A, Tharp GK, Maner-Smith K, Burd EM, Schaeffer M *et al* (2018) Caspase-8 collaborates with Caspase-11 to drive tissue damage and execution of endotoxic shock. *Immunity* 49: 42 – 55.e6

Maniscalco V, Abu-Rumeileh S, Mastrolia MV, Marrani E, Maccora I, Pagnini I, Simonini G (2020) The off-label use of anakinra in pediatric systemic autoinflammatory diseases. *Ther Adv Musculoskelet Dis* 12: 1759720X20959575

Manthiram K, Zhou Q, Aksentijevich I, Kastner DL (2017) The monogenic autoinflammatory diseases define new pathways in human innate immunity and inflammation. *Nat Immunol* 18: 832 – 842

Marsh RA, Madden L, Kitchen BJ, Mody R, McClimon B, Jordan MB, Bleesing JJ, Zhang K, Filipovich AH (2010) XIAP deficiency: a unique primary immunodeficiency best classified as X-linked familial hemophagocytic lymphohistiocytosis and not as X-linked lymphoproliferative disease. *Blood* 116: 1079 – 1082

Martinon F, Pétrilli V, Mayor A, Tardivel A, Tschopp J (2006) Gout-associated uric acid crystals activate the NALP3 inflammasome. *Nature* 440: 237 – 241

Mehta P, Cron RQ, Hartwell J, Manson JJ, Tattersall RS (2020) Silencing the cytokine storm: the use of intravenous anakinra in haemophagocytic lymphohistiocytosis or macrophage activation syndrome. *Lancet Rheumatol* 2: e358 – e367

Menu P, Vince JE (2011) The NLRP3 inflammasome in health and disease: the good, the bad and the ugly. *Clin Exp Immunol* 166: 1 – 15

Mokry LE, Zhou S, Guo C, Scott RA, Devey L, Langenberg C, Wareham N, Waterworth D, Cardon L, Sanseau P *et al* (2019) Interleukin-18 as a drug repositioning opportunity for inflammatory bowel disease: a mendelian randomization study. *Sci Rep* 9: 9386

Monteleone G, Trapasso F, Parrello T, Biancone L, Stella A, Iuliano R, Luzza F, Fusco A, Pallone F (1999) Bioactive IL-18 expression is up-regulated in Crohn's disease. *J Immunol* 163: 143 – 147

Mudde ACA, Booth C, Marsh RA (2021) Evolution of our understanding of XIAP deficiency. *Front Pediatr* 9: 660520

Muendlein HI, Jetton D, Connolly WM, Eidell KP, Magri Z, Smirnova I, Poltorak A (2020) cFLIPL protects macrophages from LPS-induced pyroptosis via inhibition of complex II formation. *Science* 367: 1379 – 1384

Murphy JM, Czabotar PE, Hildebrand JM, Lucet IS, Zhang JG, Alvarez-Diaz S, Lewis R, Lalaoui N, Metcalf D, Webb AI *et al* (2013) The Pseudokinase MLKL mediates necroptosis via a molecular switch mechanism. *Immunity* 39: 443 – 453

Nielsen OH, LaCasse EC (2017) How genetic testing can lead to targeted management of XIAP deficiency-related inflammatory bowel disease. *Genet Med* 19: 133 – 143

Nunes T, Bernardazzi C, de Souza HS (2014) Cell death and inflammatory bowel diseases: apoptosis, necrosis, and autophagy in the intestinal epithelium. *Biomed Res Int* 2014: 218493

Orning P, Weng D, Starheim K, Ratner D, Best Z, Lee B, Brooks A, Xia S, Wu H, Kelliher MA *et al* (2018) Pathogen blockade of TAK1 triggers caspase-8-dependent cleavage of gasdermin D and cell death. *Science* 362: 1064 – 1069

Parackova Z, Milota T, Vrabcova P, Smetanova J, Svaton M, Freiberger T, Kanderova V, Sediva A (2020) Novel XIAP mutation causing enhanced spontaneous apoptosis and disturbed NOD2 signalling in a patient with atypical adult-onset Crohn's disease. *Cell Death Dis* 11: 430

Patankar JV, Becker C (2020) Cell death in the gut epithelium and implications for chronic inflammation. *Nat Rev Gastroenterol Hepatol* 17: 543 – 556

Quaranta M, Wilson R, Goncalves Serra E, Pandey S, Schwerd T, Gilmour K, Klenerman P, Powrie F, Keshav S, Travis SPL *et al* (2018) Consequences of identifying XIAP deficiency in an adult patient with inflammatory bowel disease. *Gastroenterology* 155: 231 – 234

Rapp UR, Cleveland JL, Fredrickson TN, Holmes KL, Morse HC 3rd, Jansen HW, Patschinsky T, Bister K (1985) Rapid induction of hemopoietic neoplasms in newborn mice by a raf(mil)/myc recombinant murine retrovirus. *J Virol* 55: 23 – 33

Rashidi M, Wicks IP, Vince JE (2020) Inflammasomes and cell death: common pathways in microparticle diseases. *Trends Mol Med* 26: 1003 – 1020

Rogers C, Fernandes-Alnemri T, Mayes L, Alnemri D, Cingolani G, Alnemri ES (2017) Cleavage of DFNA5 by caspase-3 during apoptosis mediates progression to secondary necrotic/pyroptotic cell death. *Nat Commun* 8: 14128

Ruhl S, Broz P (2015) Caspase-11 activates a canonical NLRP3 inflammasome by promoting K(+) efflux. *Eur J Immunol* 45: 2927 – 2936

Sagulenko V, Vitak N, Vajjhala PR, Vince JE, Stacey KJ (2017) Caspase-1 is an apical caspase leading to Caspase-3 cleavage in the AIM2 inflammasome response, independent of Caspase-8. *J Mol Biol* 430: 238 – 247

Sarhan J, Liu BC, Muendlein HI, Li P, Nilson R, Tang AY, Rongvaux A, Bunnell SC, Shao F, Green DR *et al* (2018) Caspase-8 induces cleavage of gasdermin D to elicit pyroptosis during Yersinia infection. *Proc Natl Acad Sci U S A* 115: E10888 – E10897

Sborgi L, Ruhl S, Mulvihill E, Pipercevic J, Heilig R, Stahlberg H, Farady CJ, Muller DJ, Broz P, Hiller S (2016) GSDMD membrane pore formation constitutes the mechanism of pyroptotic cell death. *EMBO J* 35: 1766 – 1778

Shi J, Zhao Y, Wang K, Shi X, Wang Y, Huang H, Zhuang Y, Cai T, Wang F, Shao F (2015) Cleavage of GSDMD by inflammatory caspases determines pyroptotic cell death. *Nature* 526: 660 – 665

Shouval DS, Biswas A, Kang YH, Griffith AE, Konnikova L, Mascanfroni ID, Redhu NS, Frei SM, Field M, Doty AL *et al* (2016) Interleukin 1beta mediates intestinal inflammation in mice and patients with interleukin 10 receptor deficiency. *Gastroenterology* 151: 1100 – 1104

Silke J, Vince J (2017) IAPs and cell death. *Curr Top Microbiol Immunol* 403: 95 – 117

Simpson DS, Pang J, Weir A, Kong IY, Fritsch M, Rashidi M, Cooney JP, Davidson KC, Speir M, Djajawi TM *et al* (2022) Interferon-gamma primes macrophages for pathogen ligand-induced killing via a caspase-8 and mitochondrial cell death pathway. *Immunity* 55: 423 – 441

Speckmann C, Ehl S (2014) XIAP deficiency is a mendelian cause of late-onset IBD. *Gut* 63: 1031 – 1032

Speir M, Lawlor KE (2021) RIP-roaring inflammation: RIPK1 and RIPK3 driven NLRP3 inflammasome activation and autoinflammatory disease. *Semin Cell Dev Biol* 109: 114 – 124

Strigli A, Gopalakrishnan S, Zeissig Y, Basic M, Wang J, Schwerd T, Doms S, Peuker K, Hartwig J, Harder J *et al* (2021) Deficiency in X-linked inhibitor of apoptosis protein promotes susceptibility to microbial triggers of intestinal inflammation. *Sci Immunol* 6(65). https://doi.org/10.1126/sciimmunol.abf7473

Takada H, Nomura A, Ohga S, Hara T (2001) Interleukin-18 in hemophagocytic lymphohistiocytosis. *Leuk Lymphoma* 42: 21 – 28

Tang YM, Xu XJ (2011) Advances in hemophagocytic lymphohistiocytosis: pathogenesis, early diagnosis/differential diagnosis, and treatment. *ScientificWorldJournal* 11: 697 – 708

Uren AG, Pakusch M, Hawkins CJ, Puls KL, Vaux DL (1996) Cloning and expression of apoptosis inhibitory protein homologs that function to inhibit apoptosis and/or bind tumor necrosis factor receptor-associated factors. *Proc Natl Acad Sci U S A* 93: 4974 – 4978

de Vasconcelos NM, Van Opdenbosch N, Van Gorp H, Martin-Perez R, Zecchin A, Vandenabeele P, Lamkanfi M (2020) An apoptotic caspase network safeguards cell death induction in pyroptotic macrophages. *Cell Rep* 32: 107959

Verhagen AM, Ekert PG, Pakusch M, Silke J, Connolly LM, Reid GE, Moritz RL, Simpson RJ, Vaux DL (2000) Identification of DIABLO, a mammalian protein that promotes apoptosis by binding to and antagonizing IAP proteins. *Cell* 102: 43 – 53

Vince JE, Silke J (2016) The intersection of cell death and inflammasome activation. *Cell Mol Life Sci* 73: 2349 – 2367

Vince JE, Wong WW, Khan N, Feltham R, Chau D, Ahmed AU, Benetatos CA, Chunduru SK, Condon SM, McKinlay M *et al* (2007) IAP antagonists target cIAP1 to induce TNFalpha-dependent apoptosis. *Cell* 131: 682 – 693

Vince JE, Wong WW, Gentle I, Lawlor KE, Allam R, O'Reilly L, Mason K, Gross O, Ma S, Guarda G *et al* (2012) Inhibitor of apoptosis proteins limit RIP3 kinase-dependent interleukin-1 activation. *Immunity* 36: 215 – 227

Vince JE, De Nardo D, Gao W, Vince AJ, Hall C, McArthur K, Simpson D, Vijayaraj S, Lindqvist LM, Bouillet P *et al* (2018) The mitochondrial apoptotic effectors BAX/BAK activate Caspase-3 and -7 to trigger NLRP3 inflammasome and Caspase-8 driven IL-1beta activation. *Cell Rep* 25: 2339 – 2353.e34

Wada T, Kanegane H, Ohta K, Katoh F, Imamura T, Nakazawa Y, Miyashita R, Hara J, Hamamoto K, Yang X *et al* (2014) Sustained elevation of serum

interleukin-18 and its association with hemophagocytic lymphohistiocytosis in XIAP deficiency. *Cytokine* 65: 74 – 78

Wahida A, Müller M, Hiergeist A, Popper B, Steiger K, Branca C, Tschurtschenthaler M, Engleitner T, Donakonda S, De Coninck J *et al* (2021) XIAP restrains TNF-driven intestinal inflammation and dysbiosis by promoting innate immune responses of Paneth and dendritic cells. *Sci Immunol* 6(65). https://doi.org/10.1126/sciimmunol.abf7235

Wang Y, Gao W, Shi X, Ding J, Liu W, He H, Wang K, Shao F (2017) Chemotherapy drugs induce pyroptosis through caspase-3 cleavage of a gasdermin. *Nature* 547: 99 – 103

Wang C, Yang T, Xiao J, Xu C, Alippe Y, Sun K, Kanneganti TD, Monahan JB, Abu-Amer Y, Lieberman J *et al* (2021) NLRP3 inflammasome activation triggers gasdermin D-independent inflammation. *Sci Immunol* 6: eabj3859

Weiss ES, Girard-Guyonvarc'h C, Holzinger D, de Jesus AA, Tariq Z, Picarsic J, Schiffrin EJ, Foell D, Grom AA, Ammann S *et al* (2018) Interleukin-18 diagnostically distinguishes and pathogenically promotes human and murine macrophage activation syndrome. *Blood* 131: 1442 – 1455

Wicki S, Gurzeler U, Wei-Lynn Wong W, Jost PJ, Bachmann D, Kaufmann T (2016) Loss of XIAP facilitates switch to TNFalpha-induced necroptosis in mouse neutrophils. *Cell Death Dis* 7: e2422

Wong WW, Vince JE, Lalaoui N, Lawlor KE, Chau D, Bankovacki A, Anderton H, Metcalf D, O'Reilly L, Jost PJ *et al* (2014) cIAPs and XIAP regulate myelopoiesis through cytokine production in an RIPK1- and RIPK3-dependent manner. *Blood* 123: 2562 – 2572

Worthey EA, Mayer AN, Syverson GD, Helbling D, Bonacci BB, Decker B, Serpe JM, Dasu T, Tschannen MR, Veith RL *et al* (2011) Making a definitive diagnosis: successful clinical application of whole exome sequencing in a child with intractable inflammatory bowel disease. *Genet Med* 13: 255 – 262

Yabal M, Muller N, Adler H, Knies N, Gross CJ, Damgaard RB, Kanegane H, Ringelhan M, Kaufmann T, Heikenwalder M *et al* (2014) XIAP restricts TNF- and RIP3-dependent cell death and inflammasome activation. *Cell Rep* 7: 1796 – 1808

Zeissig Y, Petersen BS, Milutinovic S, Bosse E, Mayr G, Peuker K, Hartwig J, Keller A, Kohl M, Laass MW *et al* (2015) XIAP variants in male Crohn's disease. *Gut* 64: 66 – 76

Zhang Y, Maksimovic J, Huang B, De Souza DP, Naselli G, Chen H, Zhang L, Weng K, Liang H, Xu Y *et al* (2018) Cord blood CD8(+) T cells have a natural propensity to express IL-4 in a fatty acid metabolism and caspase activation-dependent manner. *Front Immunol* 9: 879

Expanded View Figures

Figure EV1. XIAP deficiency abrogates NOD2 signalling.

A Sanger-sequencing confirming XIAP frameshift (T933del-AGAAC) in patient 1 and a misssense mutation (c.595C>T:p.Q199X) in patient 2.

B Colonoscopy images of the XIAP-deficient patients at diagnosis.

C, D ELISA analysis of IL-6 and TNF in PBMC supernatants upon NOD2 ligand muramyl dipeptide (10 μg/ml) stimulation for 24 h. The mean of duplicate experiments is shown.

E Paraffin-embedded sections of colonic biopsies were stained with secondary Alexa fluor anti-rabbit 594 and or anti-mouse 488.

F, G BMDMs were seeded at a density of 4×10^5 cells per well, primed with 20 ng/ml of LPS for 6 h then treated, as indicated, with 500 nM of the indicated smac-mimetic compounds for 20 h. Cell viability (F) was determined by PI staining and flow cytometry and measured as a proportion of PI-negative (live) cells. Data represent the mean of three independent experiments (symbols). Error bars are the mean ± SD. Alternatively, cell lysates were analysed by western blot (G). Data representative of two independent experiments.

Source data are available online for this figure.

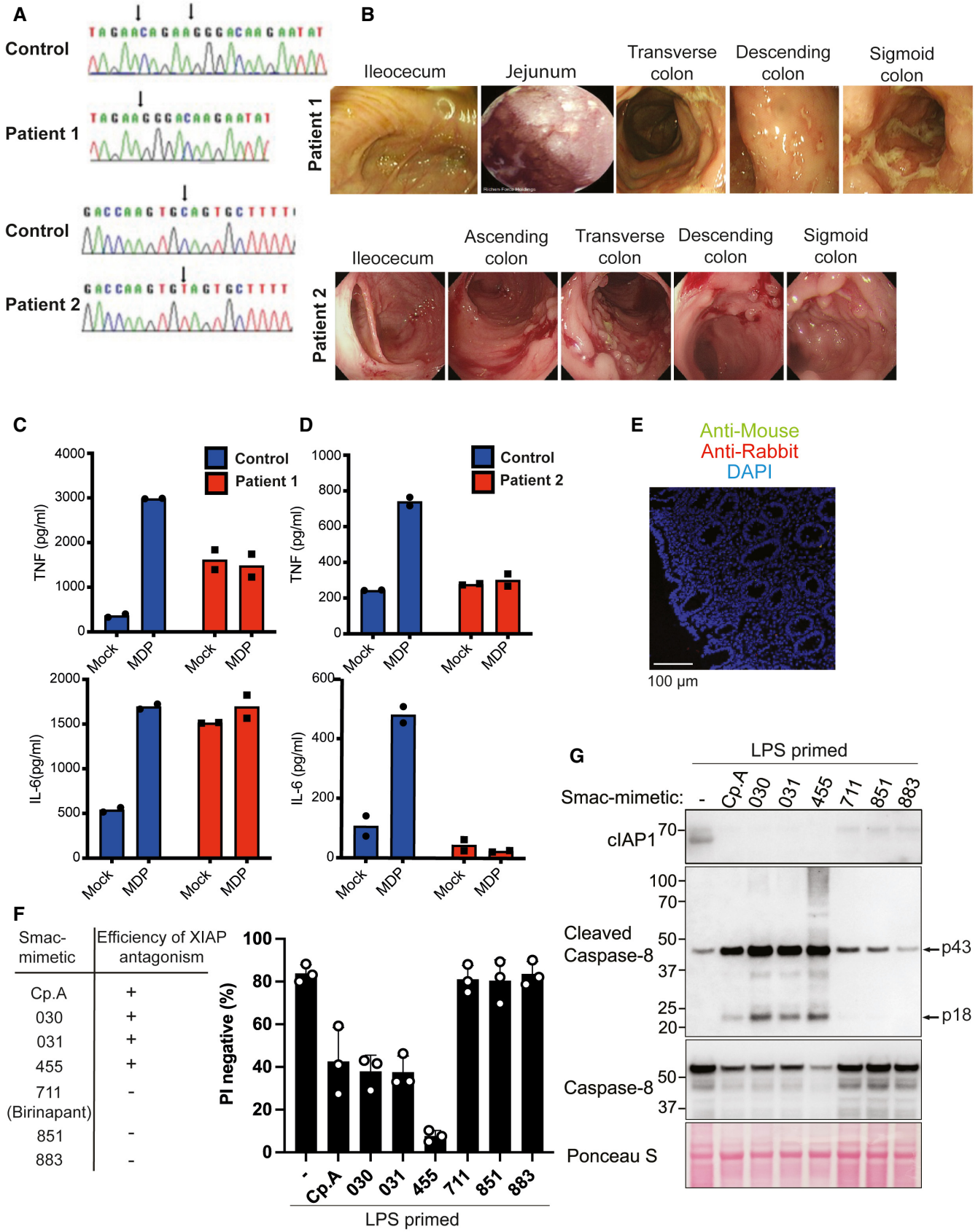
A
Control
Patient 1
Control
Patient 2
B
Ileocecum
Jejunum
Transverse colon
Descending colon
Sigmoid colon
Patient 1
Ileocecum
Ascending colon
Transverse colon
Descending colon
Sigmoid colon
Patient 2
C
Control
Patient 1
TNF (pg/ml)
IL-6(pg/ml)
Mock
MDP
D
Control
Patient 2
TNF (pg/ml)
IL-6 (pg/ml)
E
Anti-Mouse
Anti-Rabbit
DAPI
100 µm
F
Smac-mimetic
Efficiency of XIAP antagonism
Cp.A +
030 +
031 +
455 +
711 (Birinapant) -
851 -
883 -
PI negative (%)
LPS primed
G
LPS primed
Smac-mimetic: - Cp.A 030 031 455 711 851 883
cIAP1
Cleaved Caspase-8
p43
p18
Caspase-8
Ponceau S

Figure EV1.

Figure EV2. Loss of GSDMD and GSDME does not prevent caspase-8-mediated cell death upon IAP loss or TAK1 inhibition.

A–C BMDMs of the indicated genotypes were seeded at a density of 7.5×10^4 cells per well and treated with LPS alone (A) or primed with LPS (100 ng/ml) for 3 h before treatment with either Cp. A (1 μM) (B) or with Cp. A and MCC950 (5 μM) (C). Cell viability was determined through IncuCyte analysis and measured as the proportion of Cytotox Green positive cells versus SPY620-DNA positive cells. Each graph is representative of three independent experiments, data points represent the mean of triplicate wells. Error bars are the mean ± SD.

D BMDMs were seeded at a density of 4×10^5 cells per well and pre-treated with TAK1i (250 nM) for 1 h prior to the addition of LPS (100 ng/nl) for 0, 10, 20, 40 and 60 min. Cell lysates were collected and analysed by western blot. Data represent one experiment.

E, F BMDMs of the indicated genotypes were seeded at a density of 7.5×10^4 cells per well and primed with LPS (100 ng/ml) for 3 h before treatment with either TAK1i (250 nM) (E) or with TAK1i and MCC950 (5 μM) (F). Cell viability was determined through IncuCyte analysis and measured as the proportion of Cytotox Green positive cells versus SPY620-DNA positive cells. Each graph is representative of three independent experiments, data points represent the mean of triplicate wells. Error bars are the mean ± SD.

Source data are available online for this figure.

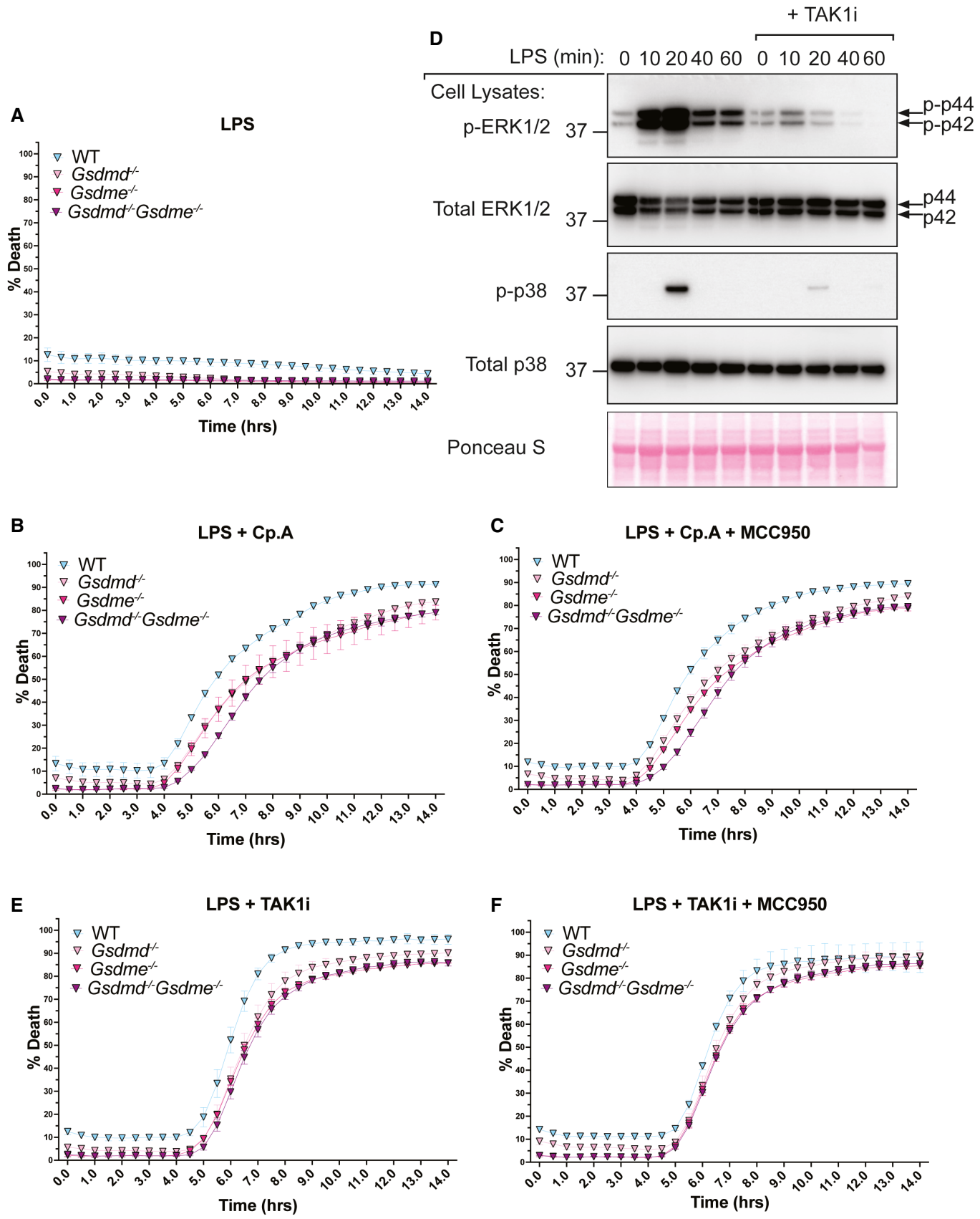
A
LPS
WT
Gsdmd-/-
Gsdme-/-
Gsdmd-/-Gsdme-/-
% Death
Time (hrs)
D
+ TAK1i
LPS (min): 0 10 20 40 60 0 10 20 40 60
Cell Lysates:
p-ERK1/2 37
p-p44
p-p42
Total ERK1/2 37
p44
p42
p-p38 37
Total p38 37
Ponceau S
B
LPS + Cp.A
C
LPS + Cp.A + MCC950
E
LPS + TAK1i
F
LPS + TAK1i + MCC950

Figure EV2.

Figure EV3. Evaluation of Caspase-3, -7 and -9 processing in BMDMs in response to apoptotic and pyroptotic stimuli.

A–D BMDMs of the indicated genotypes were seeded at a density of 4 × 105 cells per well and primed with LPS (100 ng/ml) for 3 h before treatment with Cp. A (1 μM) or TAK1i (250 nM) for 6 h, ABT-737 (1 μM) and CHX (20 μg/ml) for 4 h, or nigericin (10 μM) for 45–60 min. Cell lysates were harvested and analysed by western blot. Data represent 3 (A and C) or 2 (B and D) independent experiments.

Source data are available online for this figure.

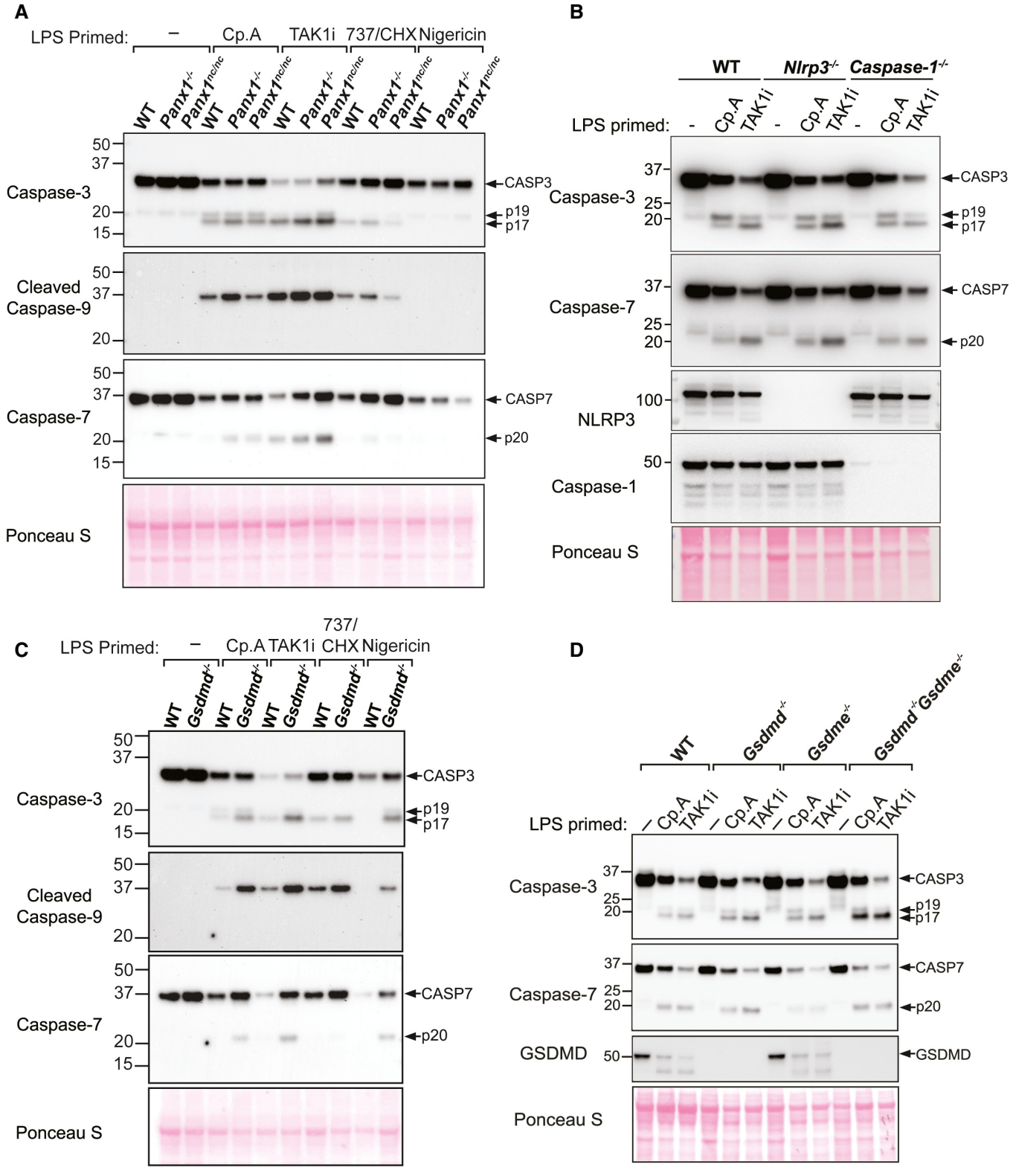
A
LPS Primed: – Cp.A TAK1i 737/CHX Nigericin
WT Panx1-/- Panx1inc/inc
Caspase-3
Cleaved Caspase-9
Caspase-7
Ponceau S
CASP3
p19
p17
CASP7
p20
B
WT Nlrp3-/- Caspase-1-/-
LPS primed: - Cp.A TAK1i
Caspase-3
Caspase-7
NLRP3
Caspase-1
Ponceau S
CASP3
p19
p17
CASP7
p20
C
LPS Primed: – Cp.A TAK1i 737/CHX Nigericin
WT Gsdmd-/-
Caspase-3
Cleaved Caspase-9
Caspase-7
Ponceau S
CASP3
p19
p17
CASP7
p20
D
WT Gsdmd-/- Gsdme-/- Gsdmd-/-Gsdme-/-
LPS primed: – Cp.A TAK1i
Caspase-3
Caspase-7
GSDMD
Ponceau S
CASP3
p19
p17
CASP7
p20
GSDMD

Figure EV3.

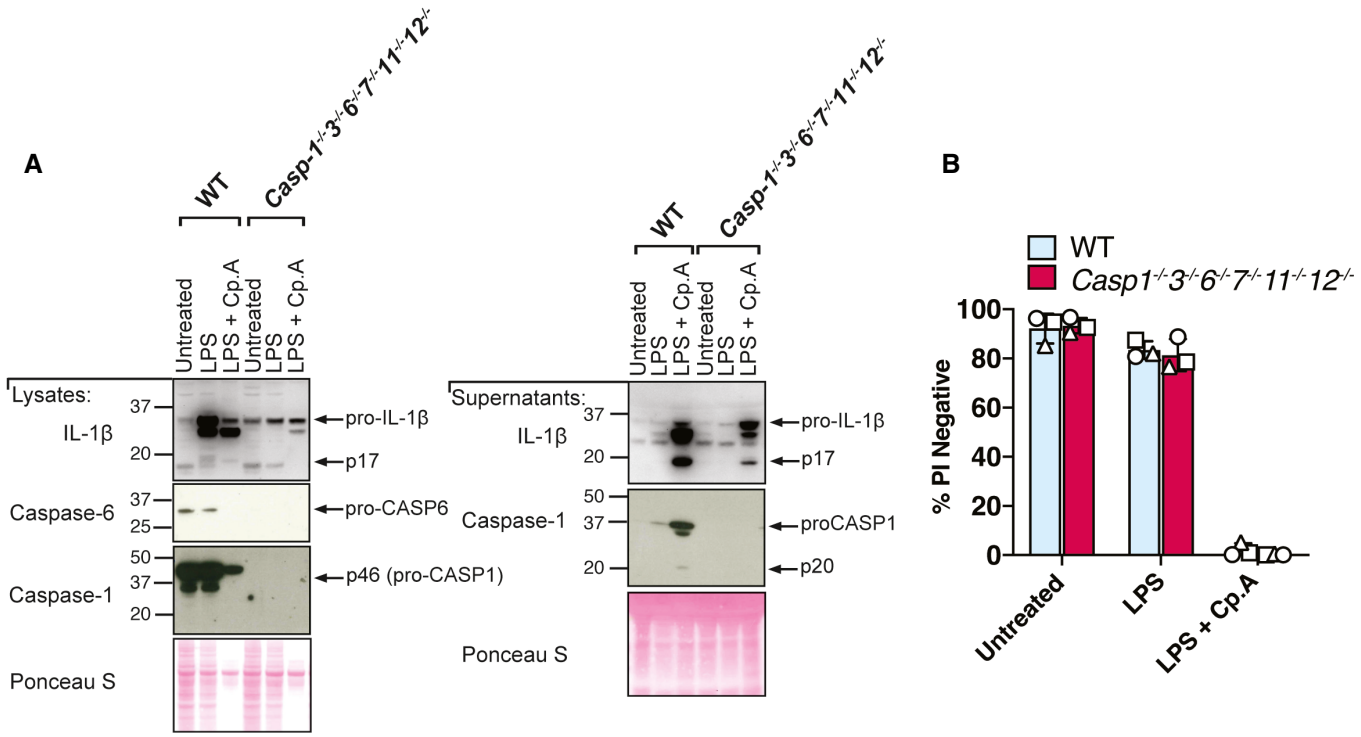

Figure EV4. In the absence of caspase-1, -3 and -7, cell death and IL-1β release upon IAP inhibition do not depend on caspase-6.

A, B iBMDMs of the indicated genotypes were seeded at a density of 3 × 105 cells per well and primed with 100 ng/ml of LPS for 3 h before treatment with Cp. A (2 μM) for 24 h. Total cell lysates and supernatants were analysed by western blot (A) or cell viability determined by propidium iodide (PI) uptake and flow cytometry (B). Data representative of three independent experiments (A), or three independent experiments (symbols) are shown (B). Error bars represent the mean ± SD.

Source data are available online for this figure.

Figure EV5. Caspase-3 and -7 deletion does not prevent fibroblast death upon IAP inhibition, and caspase-8 can process GSDMD into the p30 fore-forming fragment.

A Western blot showing CRISPR/Cas9 targeting of MCL-1 (polyclonal population) and caspase-8 processing in SV40T immortalised MEFs derived from two separate *caspase-3*$^{-/-}$*caspase-7*$^{-/-}$ (*C3*$^{-/-}$*C7*$^{-/-}$) embryos treated with or without ABT-737 (1 μM) or etoposide (34 μM) for 24 h. Data represent one experiment.

B, C SV40T immortalised MEFs of the indicated genotypes (*caspase-3*$^{-/-}$*caspase-7*$^{-/-}$ MEFs generated from two mice shown in C) were treated with ABT-737 (1 μM), etoposide (34 μM), TNF (100 ng/ml) or the IAP antagonist birinapant (1 μM) as depicted for 24 h and cell death analysed by PI uptake and flow cytometry. Three to five independent experiments (symbols) are shown. Error bars represent the mean ± SD.

D 293 T cells were transfected with the indicated cDNAs and caspase-1- or caspase-8-mediated processing of FLAG-tagged GSDMD evaluated by western blot. Ponceau staining depicts protein loading. One of two experiments.

Source data are available online for this figure.

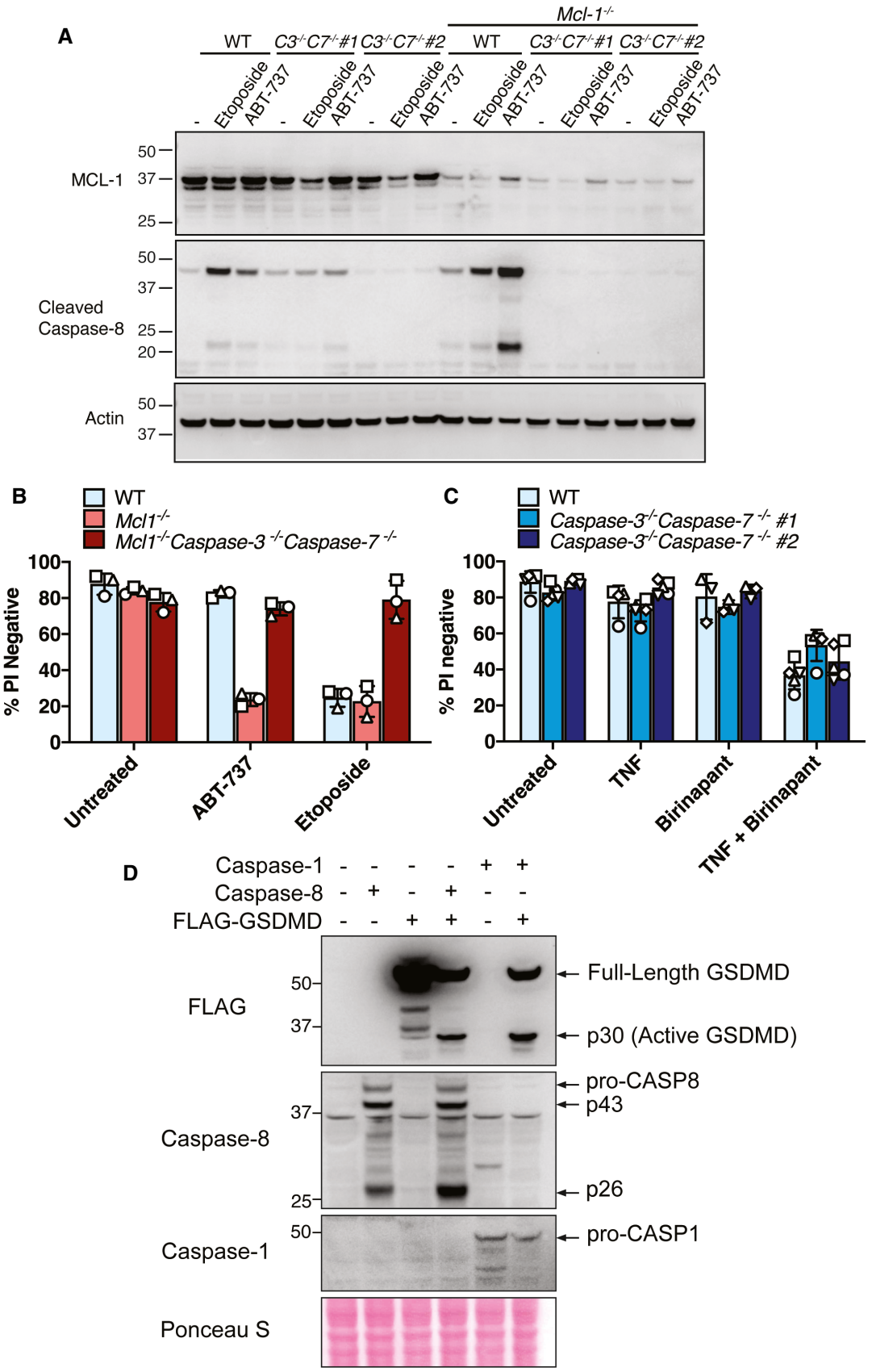
A
Mcl-1-/-
WT
C3-/-C7-/-#1
C3-/-C7-/-#2
WT
C3-/-C7-/-#1
C3-/-C7-/-#2
- Etoposide ABT-737
MCL-1
Cleaved Caspase-8
Actin
50
37
25
20
B
WT
Mcl1-/-
Mcl1-/-Caspase-3-/-Caspase-7-/-
% PI Negative
Untreated
ABT-737
Etoposide
C
WT
Caspase-3-/-Caspase-7-/- #1
Caspase-3-/-Caspase-7-/- #2
% PI negative
Untreated
TNF
Birinapant
TNF + Birinapant
D
Caspase-1
Caspase-8
FLAG-GSDMD
FLAG
Full-Length GSDMD
p30 (Active GSDMD)
Caspase-8
pro-CASP8
p43
p26
Caspase-1
pro-CASP1
Ponceau S

Figure EV5.

Appendix

Caspase-8-driven apoptotic and pyroptotic crosstalk drives cell death and IL-1β release in X-linked inhibitor of apoptosis (XIAP) deficiency

Sebastian A. Hughes *et al.*

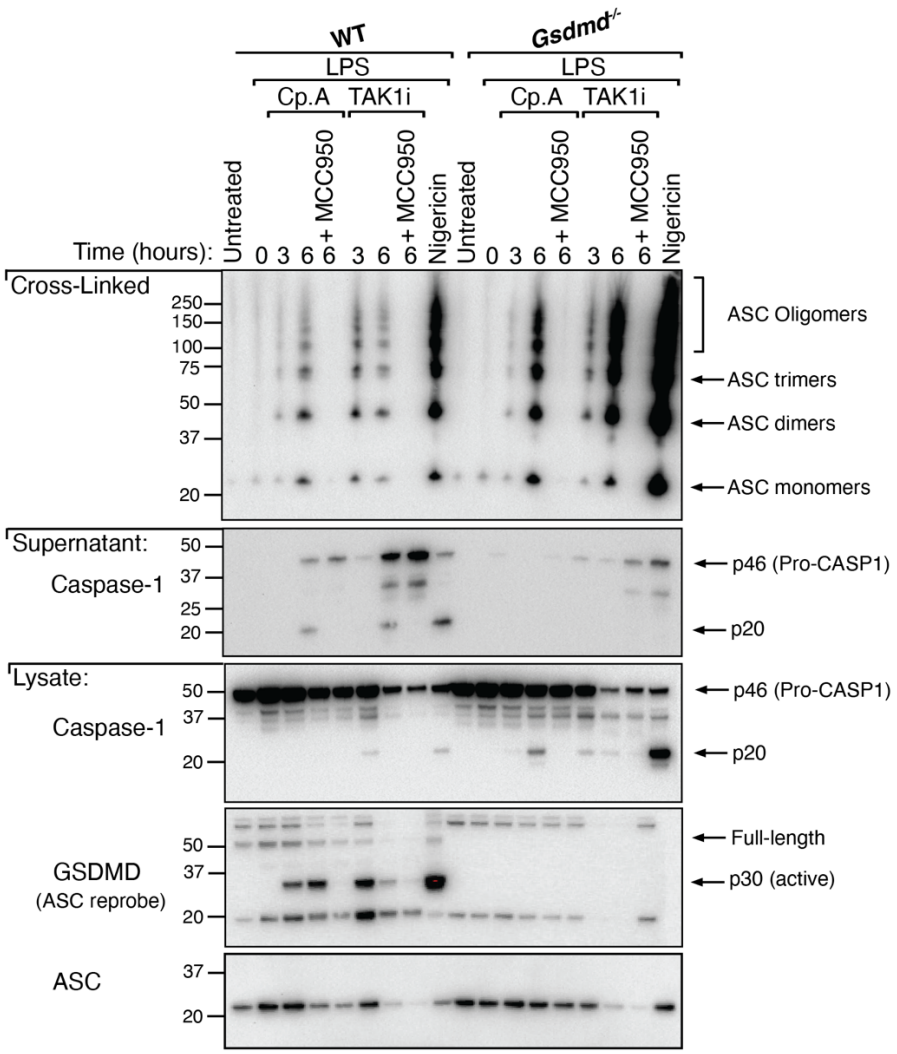

Appendix Figure S1. The deletion of GSDMD does not delay NLRP3-dependent ASC-oligomerisation upon caspase-8 activation.

BMDMs of the indicated genotypes were seeded at a density of 2 x 10^6 cell per well and primed with 100 ng/ml LPS for three hours before treatment with Cp. A (1 μM) or TAK1i (250 nM) for three and six hours. Cells were additionally treated with MCC950 (5 μM) for 30 minutes prior to treatment with Cp. A or TAK1i for six hours. PBS insoluble fractions of cell lysates were crosslinked to assess ASC-oligomerisation and these, alongside cell lysates and supernatants, were analysed by western blot. Data represents two independent experiments.

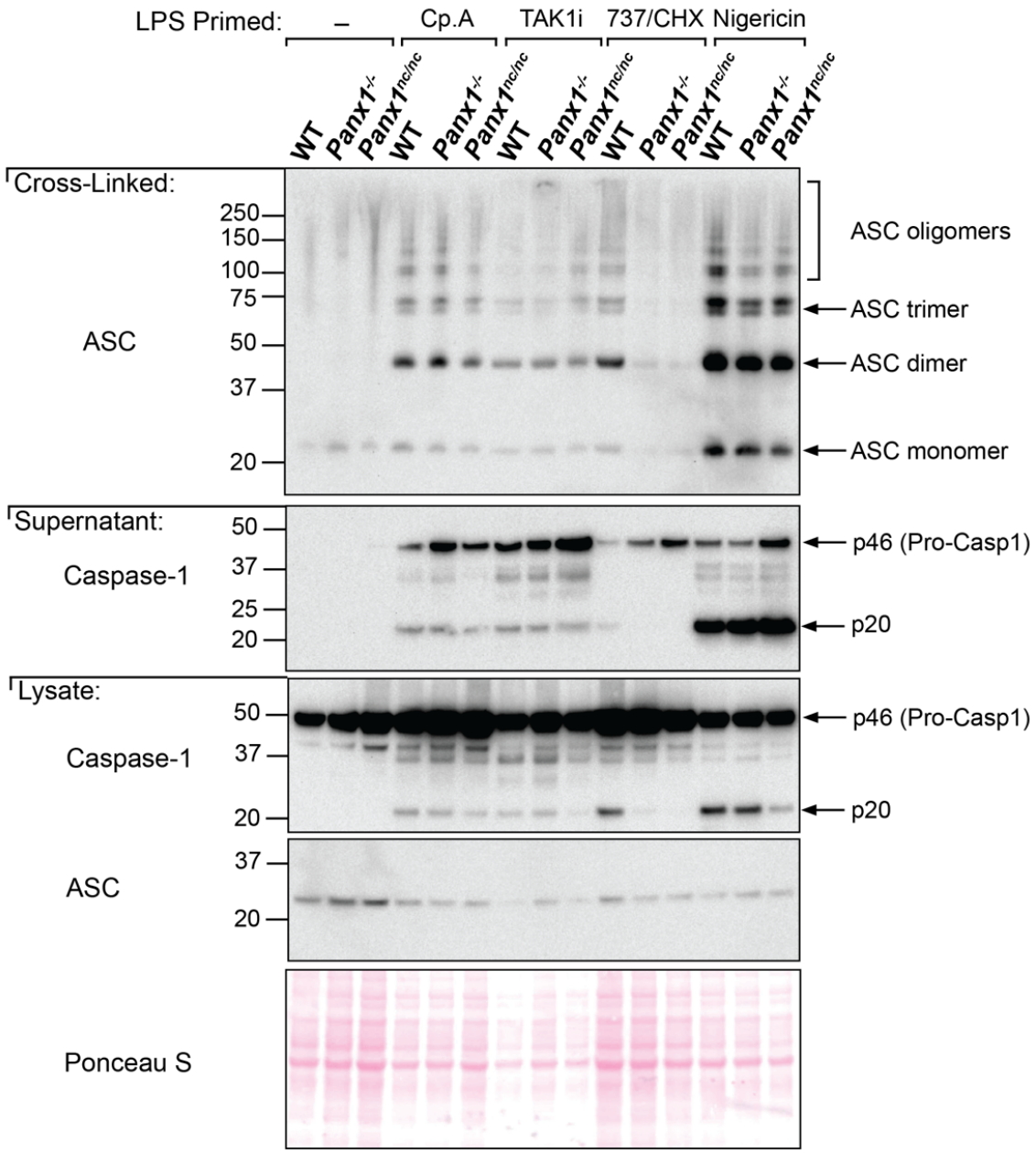

Appendix Figure S2. Pannexin-1 is required for efficient intrinsic apoptotic activation of NLRP3 but is dispensable for caspase-8-driven NLRP3 activity.
BMDMs of the indicated genotypes were seeded at a density of 2 x 10^6 cell per well and primed with 100 ng/ml LPS for three hours before treatment with Cp. A (1 μM), TAK1i (250 nM) for six hours, ABT-737 (1 μM) and CHX (20 μg/ml) for four hours, or nigericin (10 μM) for 45 minutes. Cell lysates and supernatants were then analysed by western blot. PBS insoluble fractions of cell lysates were crosslinked to assess ASC-oligomerisation and these, alongside cell lysates and supernatants, were analysed by western blot. Ponceau staining depicts protein loading. Data represents one of four independent experiments.

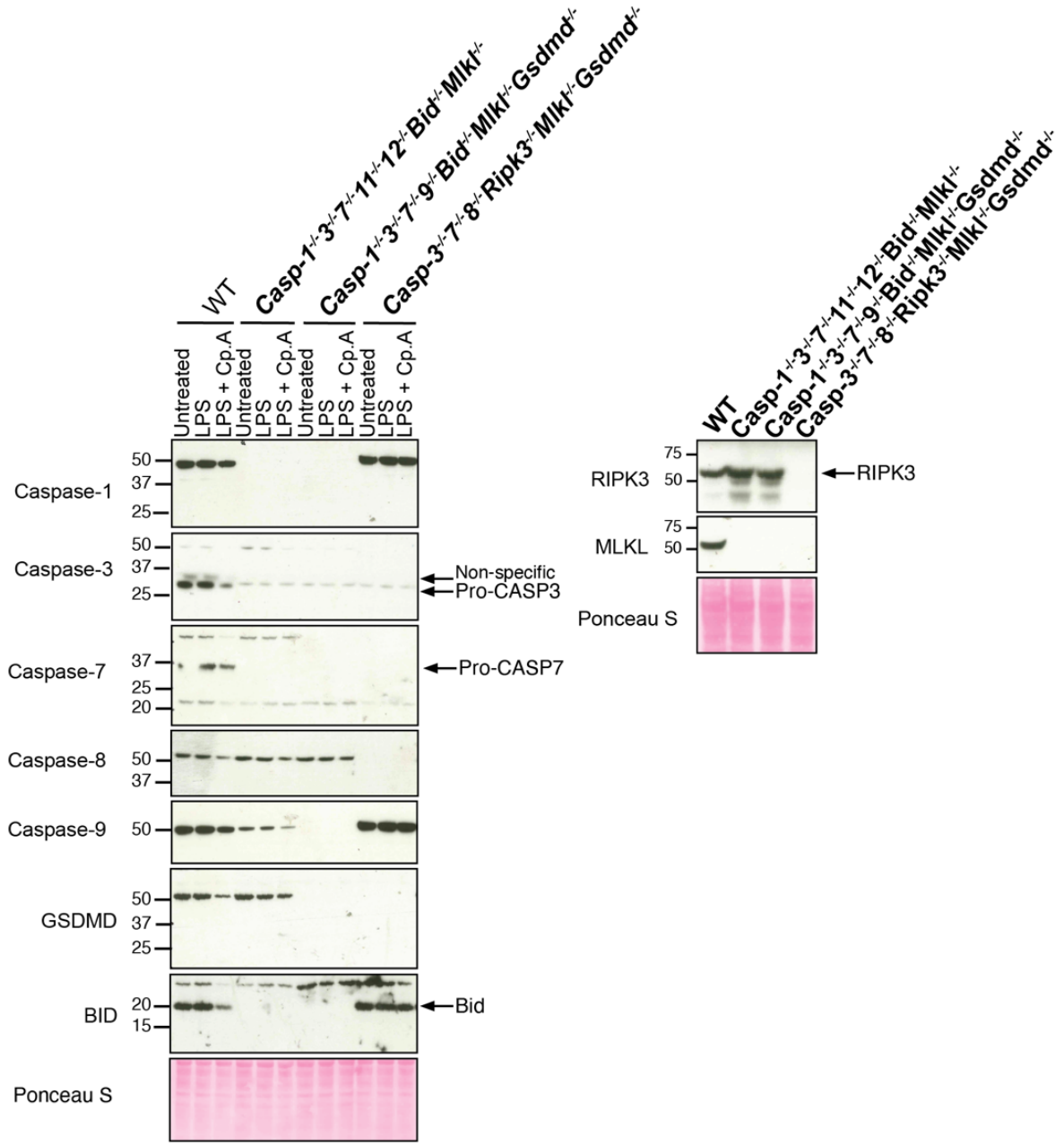

Appendix Figure S3. Validation of CRISPR/Cas9 genetic targeting of the cell death machinery in immortalised BMDMs.
iBMDMs of the indicated genotypes were primed with 50 ng/ml LPS for three hours before treatment with Cp. A (1 μM) for 24 hours as indicated and total cell lysates were then analysed by western blot. Ponceau staining depicts protein loading. One of two experiments.

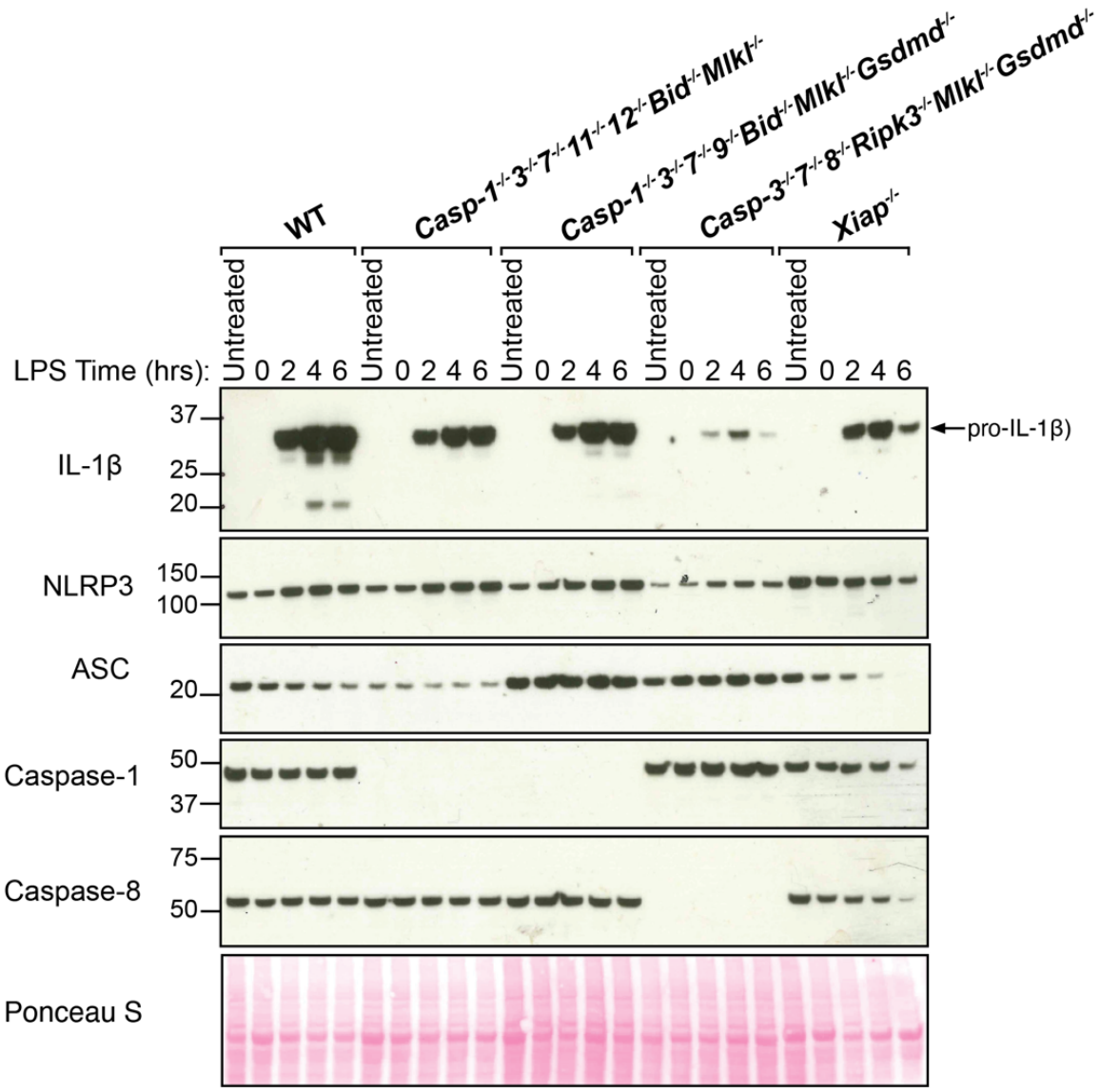

Appendix Figure S4. Evaluation of inflammasome priming in gene targeted iBMDMs. iBMDMs of the indicated genotypes were untreated or primed with LPS (100 ng/ml) for 0, 2, 4 or 6 hours and total cell lysates analysed by western blot. Ponceau staining depicts protein loading. Data represents one experiment.